universität wien

DIPLOMARBEIT

Effect of indirubin-3‘-monoxime on c-Src kinase activity in PDGF-activated vascular smooth muscle cells

angestrebter akademischer Grad

Magister der Pharmazie (Mag.pharm.)

Verfasserin / Verfasser:	Christoph GROJER
Matrikel-Nummer:	0301678
Studienrichtung /Studienzweig (lt. Studienblatt):	Pharmazie
Betreuerin / Betreuer:	Univ.-Prof. Dr. Verena Dirsch

Wien, im November 2009

Abstract

The intracellular non-receptor tyrosine kinase c-Src is crucially involved in the regulation of physiologic as well as pathologic processes including migration, proliferation, adhesion and angiogenesis. Of particular interest thereby is the participation of c-Src in PDGF-induced signalling, causing abnormal VSMC proliferation and subsequent neointima formation in the development of atherosclerosis. Possible future therapeutic approaches are therefore focusing on inhibition of abnormal VSMC proliferation by application of antiprolferative compounds.

Our main goal in this study therefore was to elicit an inhibitory effect of indirubin-3'-monoxime (I3MO), a red coloured indigo isomer used in TCM against leukaemias, on c-Src kinase as the responsible mechanism for the inhibition of PDGF-induced VSMC proliferation by I3MO.

In our first experiments we were able to reproduce the results already shown in earlier studies, when measuring the PDGF-dependent activation of the MAPK- and PI3K-pathway in the presence and absence of I3MO, whereas both signalling pathways were not affected by prior I3MO treatment. Subsequent performed measurements focusing on the PDGF-R and STAT3, a downstream target of c-Src kinase, exhibited a reduction of PDGF-R overall phosphorylation and suppression of PDGF-dependent STAT3 phosphorylation on Y^{705} under I3MO treatment of VSMCs at a 3 µM concentration, whereas regulatory phosphorylation sites of c-Src kinase (Y^{418} and Y^{529}) remained unaffected. An afterwards, in cell free environment performed *in vitro* tyrosine kinase assay with recombinant human c-Src showed decrease in c-Src kinase activity of 50 % on average.

The received resultsnindicate, that I3MO deploys an inhibitory effect onc-Src kinase, al least under *in vitro* conditions. The definite molecular mechanism causing this inhibition as well as I3MOs properties, concerning inhibition of c-Src, under cellular and *in vivo* conditions remain elusive at the moment.

Zusammenfassung

Die intrazelluläre non-receptor Tyrosin Kinase c-Src ist entscheidend in die Regulation von physiologischen und pathologischen Prozessen wie Migration, Adhäsion, Proliferation und Angiogenese involviert. Von besonderem Interesse ist dabei die Teilnahme von c-Src an PDGF-induzierten Signalwegen, welche eine übermäßige Proliferation von glatten Gefäßmuskelzellen und die anschließende Bildung einer Neointima im Rahmen der Entstehung von Atherosklerose hervorrufen.

Zukünftige therapeutische Ansätze zur Behandlung der Atherosklerose konzentrieren sich deshalb vermehrt auf die Hemmung der übermäßigen Proliferation glatter Gefäßmuskelzellen durch lokale Verabreichung von antiproliferativ wirkenden Verbindungen.

Hauptanliegen dieser Arbeit war deshalb die Hemmung der c-Src Kinase durch Indirubin-3'-monoxim (I3MO), ein rot gefärbtes Indigo Isomer welches in der TCM zur Behandlung von Leukämien verwendet wird, als verantwortlichen Mechanismus für die Hemmung der PDGF-induzierten Proliferation von glatten Gefäßmuskelzellen durch I3MO zu identifizieren.

Durch unsere ersten Experimente waren wir in der Lage die Resultate früherer Studien zu bestätigen, indem wir die Aktivierung des MAPK- und PI3K-Signalweges in Gegenwart und Abwesenheit von I3MO bestimmten, wobei keiner der beobachteten Signalwege durch vorherige Behandlung mit I3MO beeinflußt wurde.

In nachfolgenden Messungen konzentrierten wir uns auf den PDGF-Rezeptor (PDGF-R) und STAT3, ein sogenanntes „downstream target" der c-Src Kinase. Dabei zeigte sich nicht nur eine Reduktion der Gesamtphosphorylierung des PDGF-R, sondern auch eine Hemmung der Phosphorylierung von STAT3 an Y^{705} durch I3MO in einer Konzentration von 3 µM, während regulative Phosphorylierungsstellen der Kinase (Y^{418} und Y^{529}) unbeeinflußt blieben. Ein anschließend, mit rekombinanter menschlicher c-Src, durchgeführter *in vitro* Tyrosin Kinase Assay zeigte eine durchschnitttliche Reduktion der Aktivität von c-Src um etwa 50 %.

Insgesamt weisen die erzielten Resultate darauf hin, dass I3MO zumindest *in vitro* einen hemmenden Effekt auf die c-Src Kinase ausübt. Der genaue molekulare Mechanismus dieser Hemmung, sowie die Eigenschaften von I3MO unter *in vivo* Bedngungen und im Zellmodel verbleiben zu diesem Zeitpunkt jedoch unbekannt.

A CONTENTS

A CONTENTS

A CONTENTS III

B INTRODUCTION 3

1. Background 3

1.1. Aterial blood vessels 3

1.2. VSMCs in the cardiovascular system 4

2. Atherosclerosis 5

2.1. Epidemiology and risks factors 5

2.2. Pathogenesis 7

2.3. VSMCs in atherosclerosis 8

3. Platelet derived growth factor 10

3.1. Isoforms 10

3.2. Structure 10

3.3. Biosynthesis and secretion 11

3.4. PDGF receptors 11

3.5. PDGF signalling 13

3.5.1. PDGF-R autophosphorylation 14

3.5.2. PI3K pathway 15

3.5.3. PLC-γ 16

3.5.4. MAPK pathway 17

3.5.5. Signal transducers and activators of transcription 17

3.5.6. Non-receptor tyrosine kinases 18

3.5.7. Adaptor molecules in PDGF signalling 18

3.6. Physiological functions of PDGF 19

4. c-Src.....21
4.1. The Src family of tyrosine kinases 21
4.2. Source, structure and intramolecular interactions 22
4.3. Regulation of c-Src kinase activity 23
4.3.1. Regulation via tyrosine phosphorylation and dephosphorylation.....23
4.3.2. Regulation via serine and threonins dephosphorylation 25
4.3.3. Regulation via c-Src binding proteins 26
4.4. c-Src in PDGF-induced signalling 26

5. Indirubin 28
5.1. Source and origin 28
5.2. Derivatives.....28
5.3. Targets 29
5.3.1. Cyclin dependent kinases.....29
5.3.2. c-Src and STAT 3 30
5.3.3. Glykogen synthase kinase 3β.....30
5.3.4. NF-κB pathway 31
5.3.5. Aryl hydrocarbon receptor 31
5.3.6. Other targets.....32

6. Dasatinib.....33
6.1. The Philadelphia chromosome 33
6.2. Dasatinib in CML 33
6.3. Indications outside CML 34
6.4. Dasatinib resistance 34

7. Aim of the work.....35

C MATERIALS AND METHODS 39

1. Materials 39

1.1. Inhibitors 39

1.2. Recombinant proteins 39

1.3. Antioxidants 39

1.4. Antibodies 40

1.5. Buffers and solutions 41

1.6. Cell culture 44

1.7. Tyrosine kinase assay kit (chemiluminescent) 46

1.8. Equipment 47

1.9. Software 47

1.10. Consumables 48

2. Methods 49

2.1. Cell culture techniques 49

2.1.1. Cell lines 49

2.1.2. Thawing cells 49

2.1.3. Cultivation 49

2.2. Western blot 51

2.2.1. Sample preparation 51

2.2.2. Bradford protein quantification 51

2.2.3. SDS-PAGE 52

2.2.4. Western blotting 53

2.2.5. Staining of gels 53

2.2.6. Detection 54

2.3. *In vitro* tyrosine kinase assay 55

2.3.1. Principle 55

2.3.2. Procedure for enzymes in immune complexes 55

2.3.2.1. Sample preparation 55

2.3.2.2. Sample preparation with CHAPS buffer 56

2.3.2.3. Protein quantification 56

2.3.2.4. Immunoprecipitation 57

2.3.2.5. Well rehydration 57
2.3.2.6. *in vitro* kinase assay 58
2.3.2.7. Phosphotyrosine detection 59
2.3.3. Procedure for enzymes in solution 60
2.3.3.1. Well rehydration 60
2.3.3.2. Binding peptides to the plate 60
2.3.3.3. *In vitro* kinase assay 61
2.3.3.4. Phosphotyrosine detection 61
2.4. Statistics 62

D RESULTS 65

1. Effects of I3MO on Akt and Erk ½ kinases 65

2. Effects of I3MO on c-Src activation via Y^{418} and Y^{529} 67

3. Comparism of I3MO with dasatinib, a synthetic Src-/Bcr-Abl kinase inhibitor 69

4. Effect of I3MO on c-Src kinase activity 74

5. Antioxidants in PDGF signalling 85

E DISCUSSION 93

1. Introduction 93

2. PDGF-R autophosphorylation 93

3. MAPK- and PI3K-pathway 94

4. c-Src kinase 94

5. STAT 3 95

6. c-Srckinase activity 95

7. Antioxidants 96

8. Conclusion 96

F REFERENCES 101

G APPENDIX 107

1. Abbreviations 107

2. Curriculum Vitae 112

3. Acknowledgements 113

B INTRODUCTION

B INTRODUCTION

1. Background

1.1. Arterial blood vessels

Except from local adaptations, arterial blood vessels throughout the whole cardiovascular system share common wall architecture. The vessel wall consists of three concentric arranged layers: intima, media and adventitia, formed by their main cellular components: endothelial cells, smooth muscle cells and extracellular matrix (ECM), including collagen, elastin and glycosoaminoglycanes. Its innermost layer, the intima, is composed of a single layer of endothelial cells (endothelium), serving as a semipermeable membrane which allows selective transfer of small and large molecules from the lumen across the vascular wall, and minimal underlying subendothelial connective tissue. Following the intima and only separated from it by a thin membrane, the internal elastic lamina, multiple layers of alternating smooth muscle cells and connective tissue form the media. While inner parts of the media are provided with oxygen and nutrients via diffusion across the intima and the internal elastic lamina, diffusion would be insufficient for outer parts. Therefore the outer half or two third of the media are provided with oxygen via small aterioles, originating outside the vessels, the vasa vasorum. Finally, the adventitia completes the cross section of the vascular wall. It consists of connective tissue with nerve fibers, houses the vasa vasorum and is separated from the media by the external elastic lamina.[25]

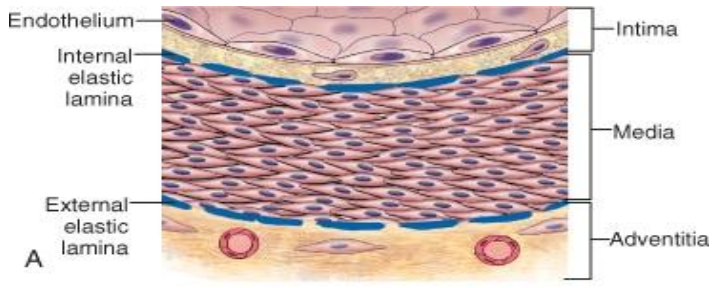

Figure 1: Schematic cross section of the vascular wall

Adapted from Kumar, V., Abbas, A.K. & Fausto, N. Pathologic basis of disease. **7th Edition**, 511 - 24 (2005)[25]

Based on size and structural differences, three types of aterial blood vessels can be defined:

- large/elastic arteries (e.g. aorta, pulmonary arteries)
- medium-sized/muscular arteries (e.g. coronary and renal arteries)
- small arteries and arterioles in tissue and organs

The structural differences of the various types are based on amount and configuration of the different components, mostly in media and ECM, depending on functional requirements of the arterial system.[25]

1.2. VSMCs in the cardiovascular system

Vascular smooth muscle cells (VSMCs) fulfil a broad variety of functions inside the cardiovascular system. Partially controlled by the autonomic nervous system, local metabolic factors and cellular interactions they regulate local blood flow and blood pressure by changing lumen size of muscular arteries and arterioles via vasodilation or vasoconstriction. VSMCs also participate in the physiologic healing process after vascular intimal injury. In response to acute EC loss, chronic endothelial injury and dysfunction VSMCs dedifferentiate while migrating from the media into the intima, allowing them to proliferate and synthesize ECM, causing intimal thickening by neointima formation. They return to a nonproliferative state, as soon as the EC layer is operable again or the level of proliferative stimuli decrease. Beside inhibitors like NO and TGF-ß, a great number of promotors like PDGF, endothellin-1, thrombin, FGF, IL-1 and IFN-γ are involved in regulating the proliferative and migratory activities of VSMCs.[25]

2. Atherosclerosis

2.1. Epidemiology and risk factors

Atherosclerosis is a common disease in developed countries with less prevalence in Central and South America, Asia and Afrika. In westerned societies atherosclerosis and its caused complications are suspected to be the reason for 50 % of all deaths. Atherosclerotic plaques preferentially develop in elastic and large – medium-sized muscular arteries supplying the heart, brain, kidneys and lower extremities. The most observed complications of atherosclerosis seem to be myocardial infarction, cerebral infarction, aortic aneurysms, peripheral vascular disease, sudden cardiac death, ischemic encephalopathy and chronic ischemic heart disease (IHD). In the last 50 years epidemiological studies were able to identify numerous risk factors with genetic or environmental background, promoting the development and progression of atherosclerosis.[25,28]

Risk factor	
High-fat/high-cholesterol diet	Appears to be the most important factor, strongly associated with the lifestyle; usually required to develop atherosclerosis in experimental animals
Smoking	Association observed in epidemiological studies; one pack or more per day over years increases death rate from IHD by 200 %; clinical studies show benefit of stopping smoking
Low antioxidant levels	Results from trials not conclusive; fat soluble antioxidants protective in experimental animals
Lack of exercise	Associated with coronary heart disease (CHD)
Infections	Epidemiological studies suggest association with various infectious agents like Chlamydia pneumoniae

Table 1: Environmentally caused risk factors for development of atherosclerosis
Adapted from: Kumar, V., Abbas, A.K. & Fausto, N.[25] and Lusis, A.J.[28]

Risk factor	
Elevated LDL/VLDL-levels	Chronic hyperlipidemia impairs EC function via production of oxygen free radicals which deactivate NO; oxidized LDL is ingested by macrophages forming foam cells, stimulates release of growth factors and cytokines, is cytotoxic to ECs and VSMCs
Reduced HDL-level	HDL physiologically mobilizes cholesterol from existing and developing atheromas and transports it to the liver for excretion
Elevated lipoprotein(a)	Altered LDL form; correlation between increased blood levels and coronary disease
Hypertension	Epidemiological studies identified it as a major risk; associated with increased risk of stroke; antihypertensive treatment reduces incidence of IHD and stroke
Homocystinuria	Causes low folate and vitamin B_6 intake, which may increase incidence of cardiovascular disease
Diabetes mellitus, type II	Induces hypercholesterolemia; increased predisposition for atherosclerosis has been shown in animal models, also increased risk for stroke and gangrene
Elevated levels of haemostatic factors	Increased fibrinogen, plasminogen activator inhibitor type 1 levels and platelet reactivity are predictors for atherosclerotic events like stroke or myocardial infarction
Depression	Associations observed in population studies
Gender	Male below 60 develop CHD twice often than women, postmenopausal women show increased incidence of atherosclerosis related diseases
Metabolic syndrome	Insulin resistance as central feature of metabolic disturbances

Table 2: Risk factors of atherosclerosis following from disease or genetic component
Adapted from: Kumar, V., Abbas, A.K. & Fausto, N. [25] and Lusis, A.J. [28]

2.2. Pathogenesis

The current understanding of the development of athersclerosis involves interaction of inflammatory and proliferative processes as response to endothelial injury. An intact endothelium is the prerequisite for maintaining vascular wall homeostasis and circulatory functions. Chronic or repetitive endothelial injury by hemodynamic forces, immune reactions, toxins, viruses, chemicals or risk factors like smoking, hypertension and hyperlipidemia lead to endothelial dysfunction, chracterized by impaired vasoreactivity, increased EC permeability and a cellular surface adhesive for inflammatory factors after expression of adhesion molecules.[11] Injured EC express VCAM-1, ICAM-1, PCAM-1, P-selectin, E-selectin and secrete MCP-1 into the vessel lumen, initially causing increased adhesion of monocytes and later on lymphocyte adhesion.[11,25,28] Due to increased endothelial permeability and stimulated by MCP-1 and other chemokines monocytes migrate into the intima, where they differentiate into macrophages and start to incorporate lipoproteins, mostly oxidized LDL, thereby becoming foam cells. Transformed intimal macrophages secrete several chemokines, growth factors and toxic oxygen species, causing other cell types to participate in the development of atherosclerotic lesions.[11]

Attracted and activated by IL-1, MCP-1 and TNF, CD4+- and CD8+-T-lymphocytes migrate into the intima, where they start to release cytokines like IFN-γ, TNF-α, TNF-ß and lymphotoxin in response to the encountered signals, resulting in activation of humoral and cellular immune mechanisms via cross-talk between macrophages and T-cells.[11] Generated oxygen species cause oxidation of LDL, which diffuses passively into the developing atherosclerotic lesion because of an increased endothelial permeability[11] and is accumulated there by apolipoprotein B – proteoglycan interactions.[28] After incorporated by intimal macrophages it causes their transformation into foam cells. Growth factors like PDGF, also released by macrophages, cause migration of VSMCs into the intima, followed by proliferation as intimal VSMCs and deposition of ECM in the atherosclerotic lesion causing intimal thickening and lesion formation. Further accumulation of foam cells, macrophages and proliferation of VSMCs accelerates progression of the initial lesion to fatty streaks and intermediate lesions and via atheroma and fibroatheroma to the final complicated lesion. Among the complications like rupture, ulceration, erosion of the

luminal surface of atheromatous plaques tresulting in thrombosis, the superimposed thrombosis and ruptured aneurysma are the most feared ones. Superimposed thrombosis occurs after thrombi are reincorporated into the neointima and occlude the vessel lumen partially or completely. Rupture of an aneurysm is the result of media weakening, caused by media atrophy and the loss of elastic tissue.[25]

Lesion type	Histology	Growth mechanism
Initial lesion (type I)	Isolated macrophage foam cells	Mainly by lipid accumulation
Fatty streak (type II)	Intracellular lipid accumulation	
Intermediate lesion (type III)	Mainly type II with small extrcellular lipid pools	
Atheroma lesion (type IV)	Mainly type II with core of extracellular lipid	
Fibroatheroma lesion (type V)	Lipid core and fibrotic layer, or multiple lipid cores and fibrotic layers, or mainly calcific, or mainly fibrotic	Accelerated smooth muscle cell proliferation and collagen increase
Complicated lesion (type VI)	Surface defect, hematoma-hemorhage, thrombus	Thrombosis, hematoma

Table 3: Classification of human atherosclerotic lesions according to the American Heart Association
Adapted from: Kumar, V., Abbas, A.K. & Fausto, N. [25]

2.3. VSMCs in atherosclerosis

The true importance of VSMCs for the development and progression of atherosclerosis is still not finally determined yet. They seem to contribute to vascular wall inflammation as well as to lipoprotein accumulation[11] and serve as cellular components for the fibrous cap and the necrotic core of atherosclerotic plaques.[25] Stimulated by growth factors like PDGF, secreted by macrophages, ECs, platelets and VSMCs themselves, and others (such as FGF, TGF-α) VSMC migrate into the intima, start to proliferate after dedifferentiation and synthesize ECM. Intimal VSMCs are also involved in maintaining the immune reaction, causing the inflammatory response necessary for progression of atherosclerotic lesions by releasing growth

factors, cytokines and chemokines (such as PDGF, bFGF, EGF, IGF-1,TGF-ß). The resulting cross talk of ECs, macrophages, T-cells and VSMCs is mainly responsible for recruitment of further inflammatory cells and VSMCs, as well as for their further paracrine activation.[11,25,28]

As cellular components of atherosclerotic plaques VSMCs are found inside the fibrous cap, together with ECM, giving the plaque necessary stability. Even in the lipid laden, necrotic core foam cells of SMC origin are found, releasing the incorporated lipids after apoptosis induced by inflammatory cells.[25]

In response to vascular injury as consequence of therapies like bypass surgery or stent implantation, VSMC undergo a proliferative response leading to in-stent restenosis, vein bypass graft failure or transplant vasculopathy. Between 30 and 40 % of patients receiving percutaneous balloon angioplasty develop restenosis within 6 months. After deployment of stents, the incidence is about 20 %, while ranging from 10 – 30 % per year after bypass surgery.[11]

3. Platelet derived growth factor

3.1. Isoforms

Originally identified as a mitogenic compound for SMCs, fibroblasts and other cell types in whole blood serum and purified from α-granules of platelets more than 2 decades ago[19,33], the today common known PDGF/VEGF family consists of 5 dimeric PDGF isoforms, 4 homodimeric (PDGF-AA, -BB, -CC, -DD) and 1 heterodimeric (PDGF-AB)[4,17], known to be synthesized and secreted by various cell types like VSMCs, fibroblasts, macrophages, leydig cells, kidney mesangial cells, ECs, T-cells and others.[19] Each of the five members is formed by disulphide-linking from 2 of the four known, from 4 different genes encoded PDGF polypeptide chains (PDGF-A, -B, -C, -D).[17,48]

3.2. Structure

The PDGF chains, forming the dimeric isoforms are polypeptides of different length; depending on splicing PDGF-A is between 196 and 211 amino acids, PDGF-B 241, PDGF-C 345 and PDGF-D 370 amino acids long.[17,48]

Except PDGF-D, all other PDGFs share a common growth factor domain of about 100 amino acids length[48], the so called PDGF/VEGF growth factor homology domain, also found in other growth factors like VEGF, TGF-ß and neural growth factor.[17] This domain contains a highly conserved pattern of 8 cysteine residues, the cysteine knot motif, involved in inter- (cysteine residue 2 and 4) and intramolecular disulphide bondings. PDGF-DD misses the 5th cysteine residue of the knot motif, while 4 additional cysteine residues were identified in PDGF-CC. Compared among each other the PDGF chains show about 25 % sequence identity, while showing 50 % sequence identity when only comparing PDGF-A and –B or PDGF-C and –D.[17]

Short N-terminal extensions, which undergo proteolytic procession for biological activation are found in the ‘classical’ PDGF- A and -B. In the ‘novel’ PDGF-C and -D the CUB-domain is found as part of their N-terminal extensions.[17] Deletion of the CUB-domain is necessary for biological activation, otherwise the domain sterically blocks the receptor binding site of the growth factor domain, not allowing full-length peptides to bind their receptors until proteolytic removal of the domain.[17,48] C-termini

of the ‘classical’ PDGFs contain mainly basic sequences involved in matrix binding, while PDGF-C and –D lack amino acid sequence extensions.[17]

3.3. Biosynthesis and secretion

Synthesized already as dimers, but inactive precursors in the endoplasmic reticulum, the four PDGFs undergo proteolytic processing for biological activation. While the ‘classical’ PDGFs are processed and activated during their exocytic pathway, extracellular processing and activation is required for the ‘novel’ PDGFs.[4,17]

PDGF-A and –B, after dimerization in the ER of producing cells, are cleaved in the trans-Golgi network for protein maturation. The enzyme responsible for maturation of pro-PDGF-A has been identified as the dibasic specific proprotein convertase (PC) furin. The enzyme converting pro-PDGF-B into PDGF-B has not been identified yet, but a related PC is supposed to be involved.[17]

PDGF-CC and –DD homodimers are secreted as inactive precursors and undergo limited extracellular proteolysis by removing the CUB-domain. Plasmin was identified to be capable to cleave off these domains in both homodimeric isoforms. Tissue plasminogen activator (tPA) on the other hand only seems to process PDGF-CC homodimers.[4,17]

3.4. PDGF receptors

The five dimeric PDGFs, as extracellular stimuli, elicit cellular responses via activation of two cell surface related receptor tyrosine kinases, PDGFR-α (α-receptors) and PDGFR-ß (ß-receptors).[18,48] Each of the receptors contains five extracellular immunoglobulin-like domains, the three outermost of them involved in ligand binding via loop formation, a transmembrane domain, a juxtamembrane domain, a splitted tyrosine kinase domain with the kinase insert domain located inbetween the two sequences of the tyrosine kinase domain, and a cytoplasmatic tail.[19,48]

Due to the dimeric character of PDGFs, each isoform is able to bind two PDGF-R at the same time. Caused by ligand binding-induced dimerization and depending on binding specifities, three dimeric PDGF-R isoforms can be formed: PDGFR-αα,

PDGFR-αß and PDGFR-ßß. Binding of the five PDGF isoforms leads to formation of various PDGFR isoforms. PDGF-AA is only able to activate PDGFR-αα, PDGF-AB can activate PDGFR-αα or PDGFR-αß, while PDGF-BB can activate all three dimeric PDGF-R isoforms. The 'novel' PDGF-CC can activate PDGFR-αα or PDGFR-αß, while PDGF-DD only activates PDGFR-ßß. [4,48]

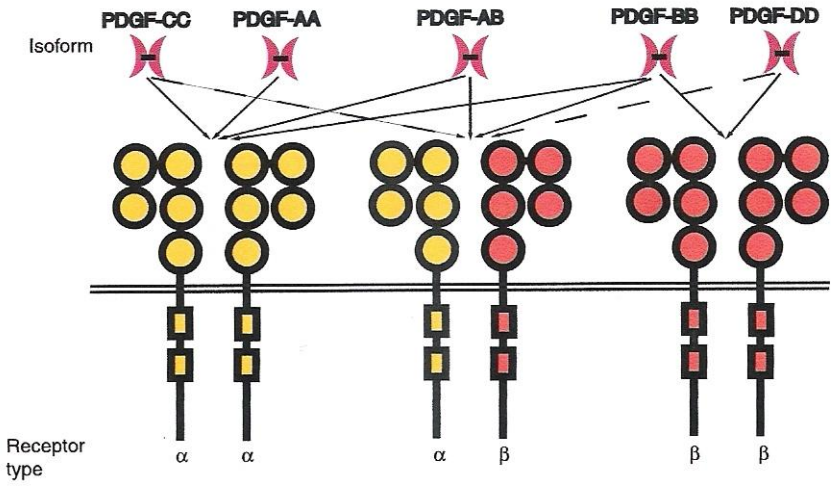

Figure 2: Interactions between the PDGF dimer and PDGFR
Each chain of the PDGF dimer interacts with a different receptor subunit. Receptor configuration is therefore depending on the ligand configuration.
Adapted from: Fredriksson, L. et al. [17]

The kind of cellular response, caused by PDGF stimulation, is therefore not only depending on the PDGF isoform acting as stimulus but also on the type of PDGF-R expressed on the cell surface. While classic target cells for PDGF, SMCs and fibroblasts express α- and ß-receptors with a generally higher amount of ß-receptors, other cells like human platelets or O-2A glial precursor cells only express α-receptors.[19]
Additional to varying PDGF-R expression in different cells types, the level of PDGF-R expression is not constant. For example, PDGFR-ß expression of connective tissue increases under inflammation, while expression of both receptors is increased under estrogen treatment. Stimulation with bFGF on the other hand causes increased expression of PDGFR-α in VSMCs. Decreased expression of PDGFR-α

can be observed under the influence of IL-1 in osteoblastic cells or in fibroblasts and mesothelial cells after TGF-ß stimulation.[19]

Cell Type	α-receptor	ß-receptor
Fibroblasts	+	+
Kidney mesangial cells	+	+
Leydig cells	+	+
Itoh cells of the liver		+
Liver sinusoidal endothelial cells	+	
Myoblasts		+
VSMCs	+	+
Capillary endothelial cells		+
Pericytes	+	
Astrocytes	+	
Neurons	+	+
Schwann cells	+	+
Mammary epithelial cells		+
Retinal pigment epithelial cells	+	
Platelets/Megakaryocytes	+	
T-cells		+
Myeloid hematopoetic cells		+
Macrophages		+

Table 4: Expression pattern of different PDGF-R in different cell types
Adapted from: Heldin, C.H., & Westermark, B. [19]

3.5. PDGF signalling

A multitude of different signalling pathways and signalling molecules is involved in mediating PDGF signals from the cellular surface into the nucleus to activate PDGF-induced cellular processes, such as cell migration, cell proliferation and transformation, by stimulating the expression of a set of intermediate early genes.

3.5.1. PDGF-R autophosphorylation

Binding of PDGF isoforms causes receptor activation by initial dimerization and adjacent autophosphorylation of the receptor complex. Phosphorylation of the receptor molecules that rather seems to occur between the dimerized receptor molecules than within each molecule (trans-phosphorylation), serves two vital purposes. While phosphorylation of Y^{857} (corresponding to Y^{849} in PDGFR-α) inside the kinase domain of PDGFR-ß is necessary to develop full kinase activity of the receptor, phosphorylation of other tyrosine residues outside of the kinase domain leads to creation of binding sites for SH2-domain-containing signalling/adaptor molecules. Eleven such autophosphorylation sites have already been identified inside the intracellular parts of the PDGFR-ß.[4,19]

Dephosphorylation of these critical tyrosine residues is a central mechanism to regulate PDGF-induced signalling. Different protein tyrosine phosphatases have been identified of being capable to dephosphorylate tyrosine residues after binding to the activated PDGF-R.[19] The best known representatives are the tyrosine phosphatases SHP-1 and SHP-2, both having two SH2 domains located in their N-termini. SHP-2 binds Y^{1009} of PDGFR-ß with high affinity and Y^{763} with lower affinity, resulting in increased phosphatase activity. For full activation both SH2 domains of the phosphatase have to be occupied. Due to its capacity as tyrosine phosphatase, SHP-2 can modulate PDGF signalling in a negative way by dephosphorylating the autophosphorylated PDGF-R and its substrates.[18]

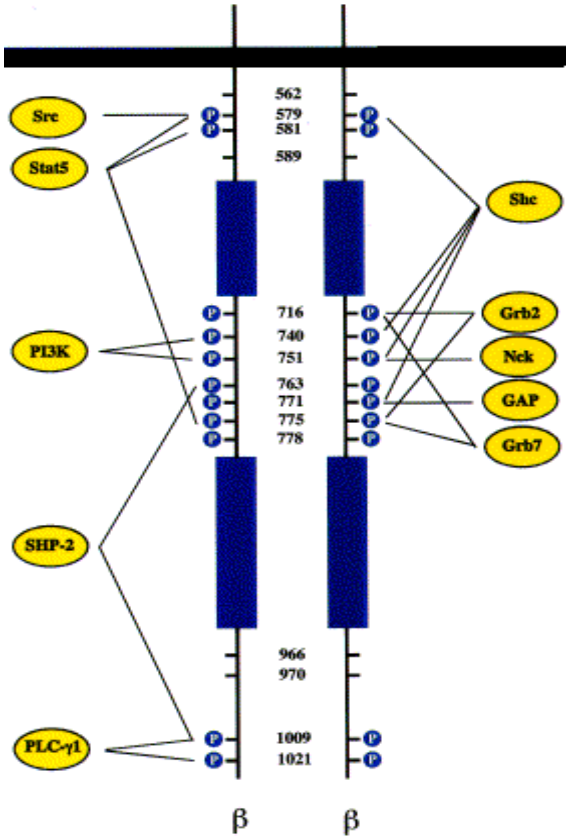

Figure 3: Identified autophosphorylation sites of PDGFR-ß

So far, 11 autophosphorylation sites of PDGFR-ß have been identified, allowing the association of SH2 domain-containing adaptor proteins or signalling molecules. Less intensively investigated, fewer autophosphorylation sites are known for PDGFR-α.

Adapted from: Heldin, C.H. et al. [19]

3.5.2. PI3K pathway

Phosphatidylinositol-3-kinase is a heterodimeric enzyme, consisting of a regulatory p85 and a catalytic p110 subunit[10,14] that can be activated by receptor tyrosine kinases as well as by non-receptor tyrosine kinases.[22] In response to PDGF stimulation the SH2 domain inside the regulatory subunit of PI3K binds to phosphorylated Y^{740} and Y^{751} of the PDGF-R leading to increased enzymatic activity due to conformational changes inside the p85 subunit and translocation of PI3K to the plasma membrane.[22] Additional direct interactions of Ras with the p110 subunit seem to be necessary to reach full enzymatic activity of PI3K.[7] Activated PI3K phosphorylates $PI(4,5)P_2$ and creates $PI(3,4,5)P_3$, which can in turn bind a number

of downstream targets containing pleckstrin-homology domains.[7,22] The major downstream target of PI3K is the serine/threonine kinase Akt. Binding of Akt to $PI(3,4,5)P_3$ recruits the kinase to the plasma membrane, where it becomes phosphorylated at T^{308} by PDK1 and at S^{473} by PDK2 to achieve full activation.[7,22] After translocation to the cytosol activated Akt phosphorylates a number of downstream targets, mostly causing their inactivation.
Phosphorylation of the Forkhead family of transcription factors (FOXO) and the apoptosis-inducing proteins BAD creates binding sites for 14-3-3 proteins. The complex of Forkhead-related transcription factor and 14-3-3 protein is therefore retained in the cytosol blocking transcription of pro-apoptotic proteins like FasL and Bim as well as cell-cycle inhibitors like p27Kip1. On the other hand Akt is capable of inhibiting p27Kip1 by direct phosphorylation. Complex formation of BAD and 14-3-3 proteins prevents BAD from binding the Bcl-2 family members Bcl-2 and Bcl-X_L, releasing them for cell survival responses.[14,22]
Another target of Akt is GSK3, a kinase necessary to keep proteins like glycogen synthase, c-Myc and cyclin D in an inactive state. Phosphorylation of GSK3 interrupts the catalytic activity of the enzyme, resulting in activation of pathways normally suppressed by active GSK3.[7,22]
Suppression of PI3K-mediated signalling is performed by SHP-1, SHP-2 and PTEN, phosphatases that dephosphorylate $PI(3,4,5)P_3$ at different positions of the inositol ring, thereby creating $PI(4,5)P_2$ and $PI(3,4)P_2$, which impair downstream signalling of PI3K.[7,14]

3.5.3. PLC-γ

Another enzyme acting on $PI(4,5)P_2$ as its preferred substrate is PLCγ. Binding of phosphorylated Y^{1021} and with lower activity Y^{1009} of PDGFR-ß leads to increased catalytic activity of PLCγ and formation of two secondary messengers, DAG and inostiol-1,4,5-triphosphate. $PI(3,4,5)P_3$ produced by PI3K and bound by PLCγ via its PH-domain is involved in another important regulatory mechanism of PLCγ activity, suggesting a cross-talk between PI3K-pathway and PLCγ.[18]

3.5.4. MAPK pathway

Activation of the small G-protein Ras by the Grb2/Sos1 complex is the initial step in induction of the MAPK-pathway. The adaptor molecule Grb2 either directly binds to phosphorylated Y^{716} of the PDGFR-ß or associates with the receptor via other adaptor molecules like Shc or SHP-2.[18] Sos1, a nucleotide exchange factor for Ras involved in the complex, switches the inactive Ras-GDP to the active Ras-GTP. Activated Ras interacts directly with the N-terminal regulatory part of the MAPKKK Raf-1, resulting in activation of the serine/threonine kinase in its C-terminal part. Raf-1 transmits the signal further by phosphorylating the dual specificity kinases MEK1/2 (MAPKKs). By phosphorylating regulatory tyrosine and threonine residues MEK1/2 finally activate the MAPKs Erk1/2 (T^{202}/Y^{204}). Erk kinases are known to phosphorylate and activate a series of transcription factors important for the regulation of cell proliferation and transformation such as Elk1, c-Fos, p53, Ets1/2 and c-Jun.[39]

Other MAPKs activated by PDGF stimulation are the c-Jun N-terminal or stress-activated protein kinases (JNK or SAPKs) and p38.[16]

Negative regulator for the MAPK pathway is the GTPase activating protein (GAP) for Ras, a molecule with two SH2 domains, able to bind phosphorylated Y^{771} of the PDGFR-ß. After binding the PDGFR-β, GAP becomes phosphorylated itself and deactivates Ras by converting it from Ras-GTP to the inactive Ras-GDP.[18]

3.5.5. Signal transducers and activators of transcription

Signal transducers and activators of transcription (STATs) are a family of cytoplasmic transcription factors currently known to consist of seven structurally related members (STAT1, STAT2, STAT3, STAT4, STAT5a, STAT5b and STAT6) and involved in signal transduction from the cellular surface to the nucleus without necessity of second messengers.[12,44] Originally assumed to be only activated by cytokines, they are actually activated by a large number of different cytokines and growth factors through phosphorylation of one single C-terminal tyrosine residue.[44,12] Phosphorylation and activation of STAT transcription factors either occurs after binding of the STAT SH2 domain to phosphorylated tyrosine residues inside the juxtamembrane domain of PDGFR-ß ($Y^{579/581}$) or is either mediated by the receptor associated family of JAK kinases (JAK 1-3, Tyk2) or intracellular non-receptor

tyrosine kinases (e.g. Src family kinases) activated by PDGF stimulation. Activated STAT molecules form homo- or heterodimeric molecules via their SH2 domains, which are immediately translocated inside the nucleus, where they regulate the expression of target genes like cyclin D1, c-myc and Bcl-X_L after binding to STAT-specific response elements (STATRE) on DNA.[41,44] By activating or repressing the transcription of these genes STATs are responsible for regulation of cellular processes like proliferation, differentiation and embryonic development. Sensitive control of duration and intensity of STAT signalling are essential to prevent development of neoplastic or autoimmune diseases, which arise from disruption or aberrant activation of STAT signalling. Therefore suppressors of cytokine signalling (SOCS) proteins serve as endogenous negative feedback regulators, these proteins bind phosphorylated receptors and non-receptor tyrosine kinases in turn preventing STAT binding and activation.[12]

3.5.6. Non-receptor tyrosine kinases

Additional signalling molecules involved in PDGF signalling are nonreceptor tyrosine kinases. Members of the Src family of tyrosine kinases (SFKs), such as Src, Fyn and Yes are cytoplasmic kinases characterised by presence of domains like SH2, SH3 or a kinase domain.[9,18] High affinity binding of SFKs SH2 domain to phosphorylated Y^{579} of PDGFR-ß and with lower affinity to Y^{581}, in combination with dephosphorylation of Y^{527} leads to increased kinase activity by disruption of tight molecular interactions.[9,18] The mechanism of c-Src tyrosine kinase activation via PDGF-R is explained in detail in section 4.3.1.
Unlike SFKs, members of the c-Fer and c-Fes cytoplasmic tyrosine kinases lack an SH3 domain and a C-terminal regulatory phosphorylation site. The importance of c-Fer and c-Fes kinases in PDGF signalling is uncertain at the moment.[18]

3.5.7. Adaptor molecules in PDGF signalling

Beside the two already mentioned adaptor molecules involved in Ras activation, Shc, mediating the association of the Grb2/Sos1 complex with PDGFR-ß and Grb2, capable of directly binding phosphorylated Y^{716} of PDGFR-ß, other adaptor molecules participate in PDGF signalling.

Nck, a small adaptor protein, consisting of one SH2 and three SH3 domains binds phosphorylated Y^{751} inside the kinase insert of PDGFR-ß and becomes itself phosphorylated on tyrosine residues, additional to already phosphorylated serine/threonine residues, after PDGF stimulation. It is supposed to be involved in activation of the JNK serine/threonine kinase by interactions with PAK1 and NIK serine/threonine kinases.[18]

Shb is an adaptor protein with a C-terminal SH2 domain and multiple proline rich sequences in the N-terminal part. After binding to phosphorylated tyrosine residues of the PDGFR-ß, Shb is presumably involved in mediating indirect interactions of PDGFR-ß and SH3 domain containing proteins.[9]

Crk, the only adaptor molecule known to bind PDGFR-α with higher affinity than PDGFR-ß, forms a complex with Cas, an SH3 domain containing protein shown to be phosphorylated after PDGF stimulation and C3G, a nucleotide exchange factor supposed to be involved in JNK activation.

The Grb7 family of adaptor proteins consists of one SH2, one PH and one domain named GM domain. Similar to Grb2, Grb7 interacts with phosphorylated Y^{716} of PDGFR-ß. Other members of this family are Grb10 and Grb14. While Grb10 binds the activated PDGFR-ß, only PDGF-stimulated serine phosphorylation of Grb14 was observed.[18]

3.6. Physiological functions of PDGF

Starting with its discovery as a mitogenic compound for mesenchymal cell types more than two decades ago, subsequent studies identified diverse other cellular processes induced by or requiring PDGF including chemotaxis, survival, apoptosis and transformation of mesenchymal cell lines.[17,48]

By using knockout or transgenic vertebrate mutants, mostly gene-targeted mice, not only the correlating *in vivo* functions of PDGF but also the different cell types targeted by PDGF were unravelled.[4]

These animal models combined with the results of the *in vitro* experiments from Heldin and Westermark identified PDGF as a growth factor with essential meaning for embryonic development, organogenesis of lung, skin, testis, kidney and lens, as well as its crucial importance for the development of the CNS, the cardiovascular and the hematopoetic system. Furthermore its involvement in blood pressure

regulation, wound healing, regulation of platelet aggregation and tissue homeostasis, and its proposed neuroprotective function make PDGF a significant participant in maintenance of physiologic processes in vertebrates and mammalians.[4]

Silencing of PDGF/PDGF-R encoding genes or selective abolition of PDGF and PDGF-R expression lead to severe abnormalities or dysfunctions of the targeted organ system or tissue, which at the worst caused death of the test animal.[4,19]

4. c-Src

4.1. The Src family kinases

c-Src, a non-receptor tyrosine kinase encoded by the c-src gene, the first proto-oncogene discovered in multicellular organisms, is the namegiving representative of a whole famly of non receptor tyrosine kinases (NRTKs) consisting of nine members: Yes, Fyn, Lyn, Lck, Hck, Fgr, Blk, Yrk and Src, commonly known as the Src family kinases.[8,43]

As signalling molecules, these multifunctional kinases regulate different cellular processes like cell differentiation, motility, proliferation, survival and adhesion by interaction with cell surface receptors (EGF-, PDGF-, FGF-receptor family, CSF-1 receptor), integrins, G-protein coupled receptors (GPCRs), steroid hormone receptors, cytokine receptors and activation of downstream signalling molecules like FAK, p85, Ras, Cas, PLC-γ and STATs either directly or via adaptor molecules ($p130^{CAS}$, Shc).[1,21]

Although essential for maintenance of physiologic cellular processes numerous members of the SFKs habe been identified to be involved in development of diseases like cancer, diabetes and others due to constitutive activation after mutation, lasting stimulation by upstream signalling molecules or defective regulation of their kinase activity.[5,21] Especially elevated levels of activated Src have been detected in various types of cancer including lung, skin, colon, breast, ovarian, endometrial cancer as well as head and neck malignancies.[21]

Just recently, the SFKs were identified as an important downstream substrate activated by Bcr-Abl kinase independent from its kinase activity in Ph^+ leukaemias, responsible for proliferation of B-lymphoid cells even after abolition of Bcr-Abl kinase activity by imatinib treatment. Considering these findings simultaneous inhibition of Bcr-Abl and SFKs seems to be the most promising approach for future Ph^+ leukaemia treatment.[26]

4.2. Source, structure and intramolecular interactions

Human c-Src is an ubiquitously expressed 60-kDa protein of 536 amino acids. Its highest protein levels are found in osteoclasts, the brain and platelets, where the expression levels are 5 – 200 fold higher than in most other cells.[35,43]

The structure of c-Src is very related to those of the other SFKs. A 14 carbon myristoyl group is attached to its N-terminal SH4 domain, mediating the commitment of c-Src to cellular membranes. Following the N-terminal SH4 domain, a poorly conserved unique domain, a 60 amino acid residue SH3 domain ,which allows the kinase to bind proline rich sequences and a 100 amino acid residue SH2 domain, allowing the enzyme to bind phosphorylated tyrosine residues, and other sequences are found.[34]

Located in between of the SH2 domain and the adjacent tyrosine kinase domain (alternatively called SH1 or catalytic domain) is the SH2-kinase linker. This motif forms the intersection between the two nearby domains and is involved in regulating c-Src kinase activity via interaction with the SH3 domain.[5]

The catalytic domain is highly conserved not only among SFKs but tyrosine kinases in general, thus it is found in kinases like Csk and PKA. Its two lobed architecture consists of a smaller N-terminal lobe (N-lobe, residues 267 – 337) mainly formed by ß-sheet structures, the larger mainly α-helical C-terminal lobe (C-lobe, residues 341 – 520) and the active site or activation loop located between them. In activated c-Src the active site of the kinase is freely accessible for ATP, allowing transfer of its γ-phosphoryl group to substrate peptides after sterical changes in the arrangement of N- and C-lobe. Giving substrates access to the active site of c-Src is not the only function these two lobes fulfil within the phosphorylation process of c-Src substrates. ATP, working as the phosphate donor, is anchored and orientated after binding the smaller N-terminal lobe of the c-Src catalytic domain, while the C-lobe works as binding site for the nucleotide-phosphate.[34,47]

The enzyme is completed by its C-terminal regulatory tail, also involved in keeping the kinase in its inactive state.[34]

This inactive conformation is typical for c-Src under normal conditions. Binding of phosphorylated Y^{527} in the C-terminal regulatory tail of c-Src (according to chicken numbering system equivalent to Y^{529} in mammalian c-Src) to the SH2 domain as well as binding of the SH2-kinase linker to the SH3 domain of c-Src stabilize the

inactive conformation with low tyrosine kinase activity. Additionally, Y^{416} (equivalent to Y^{418} in mammalian c-Src), located in the activation loop of the kinase, works as a steric barrier to avoid substrates from accessing the active site of the enzyme.[5,34] Disruption of these tight molecular interactions by dephosphorylation of Y^{527} and additional phosphorylation of ^{Y416} leads to increased kinase activity and activation of c-Src downstream signalling cascades.[5]

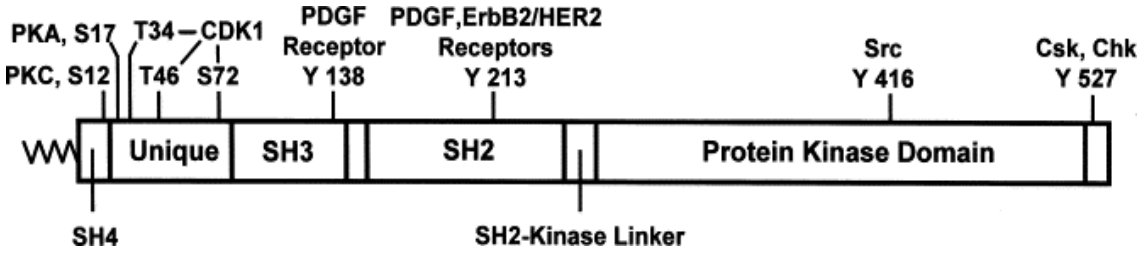

Figure 5: Phosphorylation sites and structure of c-Src kinase

Shown are the known phosphorylation sites involved in regulation of c-Src kinase activity. The different residues are labeled according to the chicken numbering system.

Adapted from: Roskoski, R. Jr. [35]

4.3. Regulation of c-Src kinase activity

The non-receptor tyrosine kinase c-Src is an essential mediator of signalling cascades required for cellular processes including proliferation, transformation, motility and adhesion. Disruption of negative regulatory mechanisms, which normally keep the kinase in an inactive state, lead to aberrant activation and increased kinase activity of c-Src and cause excessive activation of signalling pathways that regulate all stages of cancer progression.[5,21]

Regulation of c-Src kinase activity therefore is represented by tightly controlled interactions between activating and inhibitory phosphorylations of tyrosine, threonine and serine residues, mediated by various enzymes (e.g. Chk, Csk, PKA).[35]

4.3.1. Regulation via tyrosine phosphorylation and dephosphorylation

Beside others, current knowledge about c-Src identified the balance between phosphorylation and dephosphorylation of two critical tyrosine residues, Y^{416} and Y^{527}, as the main responsible mechanism for regulating the kinases activity.[34,35]

Under basal *in vivo* conditions about 90 – 95 % of Y^{527}, the negative regulator located in the C-terminal regulatory tail of c-Src, are phopshorylated. Phosphorylation of this tyrosine residue allows intramolecular binding of Y^{527} to the SH2 domain and stabilization of c-Srcs inactive conformation without tyrosine kinase activity. The first enzyme discovered to catalyze phosphorylation of Y^{527} was the cytoplasmic kinase Csk. Today several other kinases are known which are capable of suppressing c-Src kinase activity by phosphorylating Y^{527}, e.g. Chk, PKA, PKC and CDK1.[5,34] Interestingly dephosphorylation of Y^{527} alone seems to be insufficient to activate c-Src, and requires Y^{416} phosphorylation.[5]

Y^{416} is the second regulatory tyrosine residue of c-Src, located in the activation loop of its catalytic domain. In its inactive state the catalytic domain of c-Src is clenched by the SH2 and the SH3 domain, preventing Y^{416} from phosphorylation by other kinases and substrate peptides from binding to the active site of c-Src. Interception of intramolecular interactions between phosphorylated Y^{527} inside the C-terminal regulatory tail and the SH2 domain leads to disbanding of the clasp, allowing autophosphorylation of Y^{416}, which in turn causes displacement of Y^{416} from the kinases binding pocket, giving the kinase access to substrates and stabilizes the active conformation of c-Src.[5,35]

Two further tyrosine residues of minor meaning for c-Src kinase activity regulation are known, these are Y^{138} in the SH3 domain and Y^{213} in the SH2 domain of c-Src. Phosphorylation of Y^{213} is mediated by the activated PDGF-R and supposed to increase kinase activity by reducing the capability of the SH2 domain to bind phosphorylated Y^{527}. Y^{138} is also phosphorylated by the PDGF-R after association of the receptor with the SH2 domain of c-Src, causing decreased interactions between the SH3 domain and the SH2-kinase linker of c-Src.[35]

By causing the contrary effects as phosphorylation, dephosphorylation of tyrosine residues by protein tyrosine phosphatases is of the same importance for regulation of c-Src kinase activity as their phosphorylation by tyrosine kinases. Currently only PTPs capable of dephosphorylating Y^{416} and Y^{527} are known, the complexity in which these PTPs affect the phosphorylation status of Y^{138} and Y^{213} is not known presently. The phosphatases PTP1B, PTPα, PTPε, PTPλ and SHP-1 were already shown to increase c-Src kinase activity by dephosphorylation of Y^{527}.[5,35] For SHP-2, another phosphatase, an allosteric mechanism of activation was assumed beside

dephosphorylation of Y^{527}.[5] PTP-BL, the mouse homologue of human PTP-BAS, a cytosolic phosphatase, is the only PTP known of dephosphorylating Y^{416} at the moment.[35]

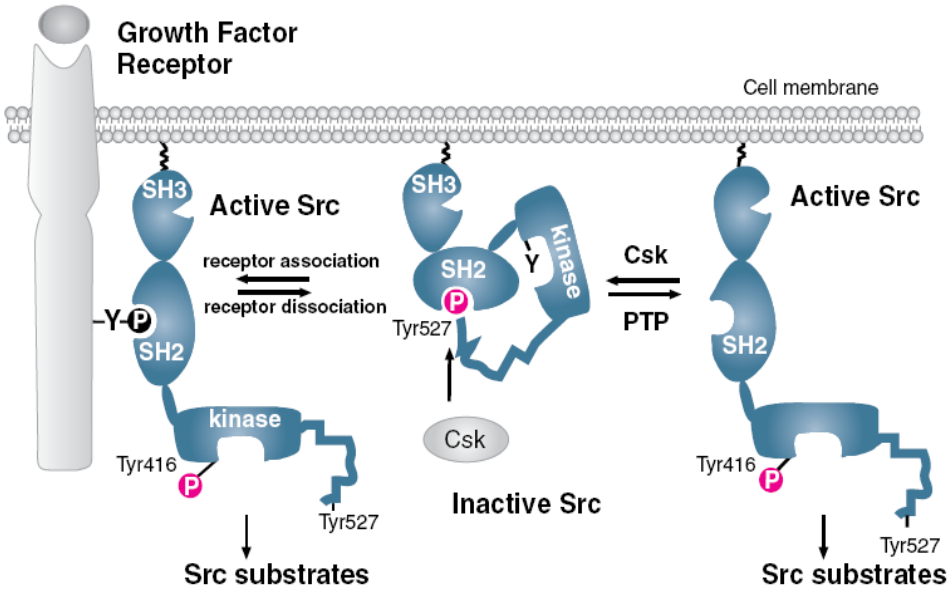

Figure 4: Regulation of c-Src kinase activity via phosphorylation of Y^{416} and Y^{527}

The kinase is normally maintained in an inactive conformation by interactions between its SH2 domain and C-terminal Y^{527}.

c-Src activation results from dephosphorylation of Y^{527} by PTPs or displacement of Y^{527} after binding of the kinases SH2 domain to autophosphorylation sites (Y^{579} and Y^{581}) of the activated PDGFR and subsequent autophosphorylation of Y^{416}. The kinase can return to its inactive state after phosphorylation of Y^{527} by Csk and other kinases or dissociation from the growth factor receptor.

Adapted from: Bjorge, J.D. et al.[5]

4.3.2. Regulation via serine and threonine phosphorylation

Aside from tyrosine kinases, c-Src is also a substrate for protein-serine/threonine kinases. Affected residues are Ser^{12} after PDGF stimulation, Ser^{17} after phosphorylation by PKA as well as Thr^{34}, Thr^{36} and Ser^{72} after phosphorylation by CDK1. The concrete mechanism of c-Src activation after phosphorylation of serine or threonine residues is still unclear today, but decreased SH2/SH3 interactions are supposed to be responsible for increased kinase activity.[35]

4.3.3. Regulation via Src-binding proteins

Src-binding proteins or adaptor proteins are a considerable element of c-Src activation. Their primary intention is to get c-Src in contact with potential substrates either by direct binding or relocalization of c-Src within the cell. But binding of different structural motifs of c-Src to these adaptor proteins has additional regulatory consequences since most of these proteins bind to sequences of c-Src that are involved in maintaining c-Src in its inactive conformation like the SH2 and SH3 domains and therefore disturb the intramolecular SH2/C-terminal tail and SH3/SH2-kinase linker interactions by competing for the same binding sites. PDGF-R and FAK bind the SH2 domain while Nef and Sin bind the SH3 domain of c-Src. $p130^{Cas}$, a protein with a large amount of binding motifs, is the only known Src-binding protein that binds the SH2 domain as well as the SH3 domain of c-Src.[5]

4.4. c-Src in PDGF-induced signalling

As for most of the PDGF-induced signalling cascades, PDGF-R dimerization and activation by autophosphorylation after ligand binding describes the initial step in activating the c-Src-dependent signalling pathway.

c-Src binds the phosphorylated tyrosine residues, Y^{579} with high affinity and Y^{581} with lower affinity, of activated PDGFR-ß with its SH2 domain, resulting in increased c-Src kinase activity by disturbing the intramolecular interactions between the kinases SH2 domain, SH3 domain, its C-terminal regulatory tail and the SH2-kinase linker, which normally keep the enzyme in its inactive conformation. Especially disturbance of the SH2 domain interactions with C-terminal phosphorylated Y^{527} seem to be crucial for activation of c-Src after PDGF stimulation. These activating mechanisms on the one hand comprise binding of the c-Src SH2 domain to phosphorylated tyrosine residues of the PDGF-R as otherwise phosphorylation of c-Src at Y^{138} and Y^{213} by the PDGF-R.[5,18]

Downstream substrate of activated c-Src is amongst others STAT3, a cytoplasmic transcription factor, serving as a key molecule in growth factor and cytokine signalling, which can be activated by RTKs like the PDGF-R as well as by NRTKs as c-Src and JAK. Members of the STAT family are involved in regulation of cellular processes via controlling expression of genes required for cell proliferation and apoptosis; target gene for STAT3 is amongst others c-myc, an intermediate early

gene. After activation by c-Src via phosphorylation on Y^{705}, STAT3 dimerizes and translocates into the nucleus, where it is responsible for modulating the expression of c-myc. Increased expression of the c-myc gene causes increased protein levels of c-Myc, a transcription factor, finally appropriate for increased DNA synthesis and mitogenesis after PDGF-dependent c-Src activation.[6]

5. Indirubin

5.1. Source and origin

The last encyclopaedia of Traditional Chinese medicine, released in 1977, enlists more than 5500 natural sources, collected by practitioners of TCM in over 4000 years of appliance, forming the basis of up to 500,000 prescriptions, today used in modern China and other countries.[20]

One of these prescriptions is Danggui Longhui Wan, a recipe consisting of 11 herbal medicines, used for the treatment of various chronic diseases, especially chronic myeloic leukaemia (CML) because of its antiproliferative effects. In 1966, the Institute of Haematology of the Chinese Academy of Medical Sciences attempted to isolate the active constituent of Danggui Longhui Wan, which was first identified as Quing Dai (indigo naturalis), a dark blue coloured powder composed of the blue dye indigo, a 2,2'-bisindole, as the main component and a small amount of the red coloured 3,2'-indigo isomer, indirubin, as minor constituent.[13,20]

Indigo naturalis, extracted from the leaves of Baphicacanthus cusia (Acanthaceae), Polygonum tinctorium (Polygonaceae), Isatis indigotinctoria (Brassicaceae), Indigofera suffrutticosa and Indigofera tinctoria (both Fabaceae), is widely used in TCM because of its hemostatic, antipyretic, anti-inflammatory, sedative, antibacterial and antiviral properties. Interestingly the antileukaemic/antproliferative qualities of indigo naturalis were not elicited by the blue indigo, but by its red coloured 3,2'-isomer indirubin.[13,20]

Both of the two compounds are produced out of the colourless precursors indican or isatan B. The evolving intermediates indoxyl and isatin finally form indigo and indirubin via dimerization and oxidation.[20]

5.2. Derivatives

Although showing good antitumor activity combined with low toxicity and missing bone marrow toxicity in animal studies as well as in studies with CML patients, indirubin is characterized by poor solubility and poor intestinal absorption. Several derivatives were synthesized to improve these pharmacological characteristics

[5-halogenoindirubin, N-ethyl-indirubin, N-methylisoindigo, indirubin-3'-monoxime (I3MO)].[13,20] Of these analogues I3MO was the most potent derivative concerning its antitumor activity. In 2007 Kim et al. were able to prove inhibition of cancer cell proliferation *in vitro* as well as a growth inhibition of solid and oral tumors *in vivo* by three novel indirubin derivatives; 5'-NIO, 5'-FIO and 5'-TAIO.[23]

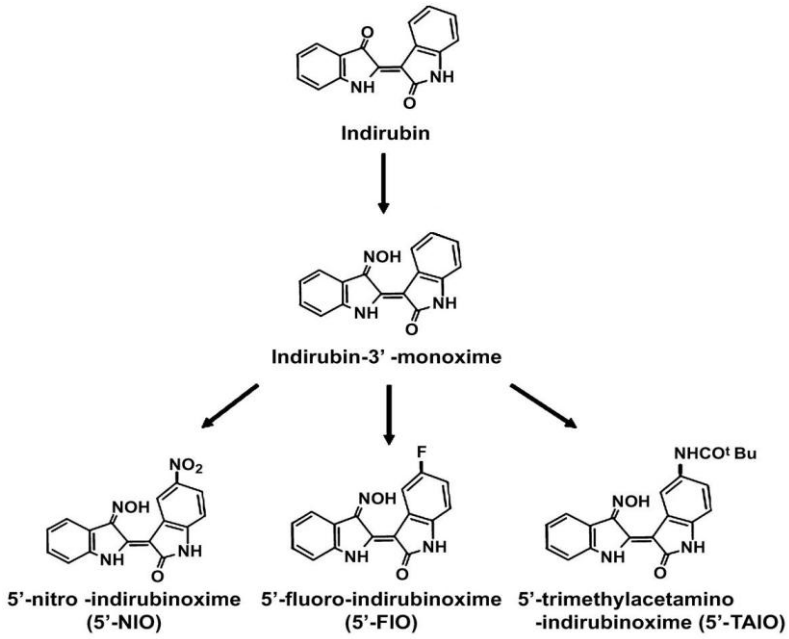

Figure 6: Chemical structure of indirubin and selected derivatives
Adapted from: Kim, S.A. et al.[23]

5.3. Targets

5.3.1. Cyclin-dependent kinases

CDKs play a crucial role in regulation of cell cycle progression. Together with their regulatory subunits, the cyclins, they form holoenzymes which hyperphosphorylate proteins serving as negative regulators of the cell cycle; one of these target proteins is the retinoblastoma protein. Hypophosphorylated pRb forms complexes with various binding partners like cAbl, HDAC, DNA polymerase δ, D type cyclins, E2F-family transcription factors and keeps them in an inactive state. Inactivation, induced

by hyperphosphorylation of pRb causes release of these transcription factors and activation of E2F-dependent transcription, necessary for S-phase progression due to the synthesis of proteins like cyclinE, cyclinA, DHFR, CDK1 and others. Today nine different CDKs and 16 corresponding cyclins are known in mammalian cells, each one of vital importance for progression through different phases of the cell cycle. Indirubin and several of its derivatives were able to inhibit cell cycle progression by binding to the ATP-binding site of different CDKs, causing G1/S-phase arrest and in concentrations $\geq$10 µM G2/M-phase arrest, accompanied by decreased pRb phosphorylation and increased apoptosis. Interestingly most of the indirubin derivatives showed higher preferences for CDK1, CDK2 and CDK5, than for CDK4, while indirubin and I3MO showed slight reduction in specificity.[13,20]

5.3.2. c-Src and STAT3

The c-Src/STAT3 cascade is one of the signalling pathways highly involved in progression of cancer. STAT3 plays an important role in tumor cell survival and proliferation via gene regulation, while c-Src acts as a key player in tumorigenesis and metastasis by activation of oncogenic signalling patways. Indirubin derivatives were able to block STAT3 signalling by direct inhibition of c-Src kinase activity (*in vitro* and *in vivo*) as well as by inhibition of tyrosine phosphorylation of STAT3 *in vivo*.[30]

5.3.3. Glykogen synthase kinase-3ß

GSK-3ß is an ubiquitously expressed serine/threonine kinase, which was originally assumed to regulate glycogen metabolism and insulin signalling, but is nowadays known as a multifunctional protein in different signalling pathways. Altogether more than 40 different proteins, including 12 transcription factors, are known to be phosphorylated by GSK-3ß. One of these proteins is ß-catenin, participant of the Wnt signalling pathway, which undergoes proteosomal degradation after phosphorylation by GSK-3ß and subsequent ubiquitination. GSK-3ß is also supposed to be involved in cell cycle progression by regulating cyclin D1 levels. Indirubin and its derivatives are known to be potent inhibitors of this enzyme supposed to be involved in the development of Alzheimer's disease.[16,46]

5.3.4. NF-κB pathway

Aside from its antiproliferative effects, indirubin shows remarkable anti-inflammatory effects through modulation of the NF-κB pathway. NF-κB is a heterotrimeric family of Rel-domain containing proteins located in the cytoplasma. Under quiescent conditions these proteins consist of a p50, p65 and IκB, a family of ankyrin-domain containing proteins (IκBα, IκBß, IκBγ, IκBε, Bcl-3, p105 and p100) required to keep NF-κB inactive. Carcinogens, inflammatory agents, tumor promoters, cigarette smoke, TNF and others activate NF-κB via activation of IKK, resulting in phosphorylation, ubiquitination and degradation of IκBα as well as phosphorylation of p65. Activated NF-κB translocates into the nucleus, binds to DNA response elements and regulates expression of antiapototic genes (cIAP1/2, survivin, TRAF, Bcl-2, Bcl-X_L), genes encoding adhesion molecules, chemokines, cytokines as well as cell cycle regulatory genes (c-myc, cyclin D1), whose products are involved in tumorigenesis. Indirubin was shown to inhibit NF-κB activation by preventing initial phosphorylation of IKK due to inhibition of TAK1, a kinase acting upstream of IKK.[37]

5.3.5. The Aryl hydrocarbon receptor

The AhR is a ligand activated transcription factor, present in most cells and tissues of the body, mediating the toxic and biological effects of dioxins. Ligand binding to the AhR causes heterodimer formation of AhR with the Aryl hydrocarbon receptor nuclear translocator followed by subsequent activation of the Ah gene battery transcription, affecting genes like CYP1A1, CYP1A2, glutathione S-transferase Ya subunit, NAD(P)H quinone oxidoreduktase, UDP-glucuronosyltransferase 1A6 and aldehyde-3-dehydrogenase genes.

In a yeast assay, indirubin showed a more potent binding to the AhR than its prototype ligand TCDD, leading to induction of CYP1A1 and 1A2 mRNA at 1 pM concentrations.[2]

5.3.6. Other targets

Other targets like tau, a kinase involved in Alzheimer's disease by formation of neurofibrillary plaques and c-Jun NH_2-terminal kinase, a regulator of neuronal cell death, make indirubin a promising new agent not only for cancer indications.[23]

6. Dasatinib

6.1. The Philadelphia chromosome

The so called Philadelphia chromosome originates from translocation [t(9,22)] of the Abl gene, typically located on chromosome 9 (der9), to chromosome 22 (der22) and subsequent replacement of a fragment of chromosome 22, adjacent to the Bcr (breakpoint cluster region) gene locus, causing the development of a Bcr-Abl fusion gene. Depending on appearing breakpoints on chromosome 22, m-Bcr (minor) and M-Bcr (major), two different Bcr-Abl fusion genes evolve. While m-Bcr leads to formation of $p185^{Bcr\text{-}Abl}$, which is a hallmark for all Ph^+-ALL, but only sporadically found in CML, M-Bcr causes formation of $p210^{Bcr\text{-}Abl}$, which is supposed to be specific for CML. The encoded fusion protein, the chimeric Bcr-Abl tyrosine kinase is constitutively activated and seems to be of pivotal importance for the development of Ph^+ leukaemias, including chronic myeloic leukaemia (CML) and B-cell acute lymphoblastic leukaemia (B-ALL).[26,32,49]

6.2. Dasatinib in CML

Developed as BMS-354825 dasatinib is an oral applied, multi-targeted Bcr-Abl and Src family kinase (SFK) inhibitor that was just recently approved by the FDA and the European Union as first-line treatment in all stages of imatinib-resistant CML. Together with nilotinib and bosutinib it forms the ‘second-generation’ of Bcr-Abl inhibitors, developed due to increased incidence of Bcr-Abl mutations leading to imatinib-resistant CML. These ‘second-generation’ inhibitors are between 20- and 325-fold more potent than imatinib, whereas dasatinib evolved the greatest potency against Bcr-Abl *in vitro* and is the only one effective against 18 of 19 known Bcr-Abl mutations leading to imatinib-resistance.[38]

Dasatinib is supposed to induce apoptosis in CML cells by inhibition of STAT5 signalling due to prior inhibition of Bcr-Abl and SFKs. Decreased DNA binding of STAT5 leads to inhibition of cell proliferation and induction of apoptosis by down regulation of STAT5 target genes like Bcl-x, Mcl-1 and cyclin D1.[31]

6.3. Indications outside CML

Although its molecular mechanism of Bcr-Abl and SFK inhibition is not totally resolved at the moment, dasatinib seems to be a promising therapeutic agent for other types of cancer as well as for Ph^+ leukaemias.

In human DU-145 cells, a very aggressive metastatic prostate cancer cell line, dasatinib inhibits cell adhesion, migration and invasion by inhibition of c-Src kinase activity and subsequent abolition of oncogenic FAK and $p130^{CAS}$ signalling.[29]

The Src/FAK/$p130^{CAS}$ signalling pathway not only seems to be involved in prostate cancer but also in other types of sarcomas, like soft tissue and bone sarcomas. In these types of malignancies dasatinib inhibited migration, invasion and induced apoptosis in an analogous manner. The only cell line not responding to dasatinib treatment was HT-1080, which was also the only one lacking detectable levels of c-Src kinase activity.[40] These findings identify dasatinib as a possible therapeutic approach against tumors exhibiting elevated Src/FAK/$p130^{CAS}$ signalling.

6.4. Dasatinib resistance

Resistance against dasatinib is mostly caused by mutations inside the Bcr-Abl kinase domain. To meet these concerns, several 'third generation' Bcr-Abl kinase inhibitors, pass through clinical development or phase I clinical trials. One of these so called 'Aurora kinase inhibitors', MK-0457, has already showed the ability to bind to dasatinib-resistant T315I-mutations of Bcr-Abl kinase. A combination study with dasatinib and MK-0457 has delivered promising outcomes to complement resistance development. If such combinations will ever be applied to CML patients is unclear at the moment.[38]

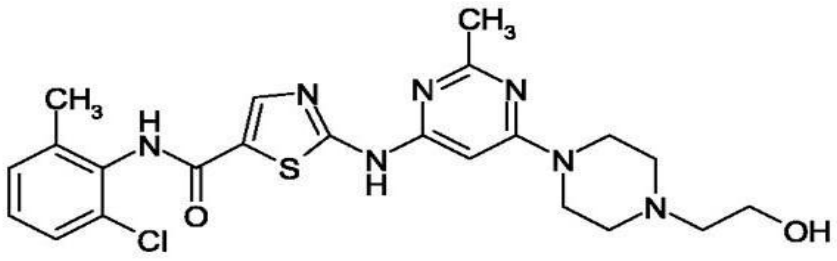

Figure 7: Chemical structure of dasatinib

Adapted from: Nam, S. et al.[29]

7. AIM OF THE WORK

Inhibition of VSMC proliferation and migration seems to be a promising therapeutic approach for the treatment of atherosclerosis, especially for the prevention of restenosis of blood vessels due to intimal thickening. To achieve this therapeutic goal compounds with sufficient antiproliferative properties against VSMCs are essential. One promising candidate seems to be indirubin, the red-coloured isomer of indigo and active principle of a TCM reciepe used for treatment of leukaemia. Due to its poor aqueos solubility several derivatives were designed, of which I3MO represents a very potent one.

Previous studies identified numerous signalling molecules inside oncogenic signalling pathways as targets for indirubin and its derivatives such as STAT3, c-Src kinase, $p130^{CAS}$ and FAK.[30,36] Additionally, these findings are of interest for the possible use as therapeutic agents against atherosclerosis, since signalling molecules like STAT3 and c-Src were also identified as participants in PDGF-induced signalling and could therefore be responsible for PDGF-dependent development of atherosclerosis due to their excessive activation.[18,19]

In previous studies a decreased autophosphorylation of the PDGF-R, abolition of STAT3 signalling and inhibition of ROS production were documented as effects of I3MO when added to VSMCs prior to PDGF stimulation.[36]

In our study we tried to identify c-Src kinase as a potential target of I3MO within the PDGF signalling cascades in VSMCs and interruption of PDGF-dependent c-Src activation as the accountable step for subsequent inhibition of STAT3 signalling. Furthermore we tried to specify the inhibitory effect of I3MO on c-Src kinase activity by performing an *in vitro* tyrosine kinase assay.

C MATERIALS AND METHODS

C MATERIALS AND METHODS

1. Materials

1.1. Inhibitors

Name	Concentration	Provider
Indirubin-3'-monoxime	3 µM	Laurent Meijer (Roscoff, France)
Dasatinib	100 nM	LC Laboratories (Woburn, MA, USA)

Table 5: Inhibitors

Inhibitor stock solutions (10 mM, dissolved in DMSO) were stored at -80°C.

1.2. Recombinant proteins

Name	Concentration	Provider
recombinant PDGF-BB, human	1 µg/µl	Bachem (Weil am Rhein, Germany)
recombinant Src, human	10 µg/100 µl	Millipore (Billeria, MA, USA)

Table 6: Recombinant proteins

PDGF-BB stock solution (10 ng/µl) was stored in 20 µl aliqouts at -20°C and diluted with starvation medium to a final concentration of 1 ng/µl before use.
Src stock solution (10 µg/100 µl) was stored at -80°C.

1.3. Antioxidants

Antioxidant	Concentration	Solvent	Provider
Ascorbic acid	100 µM	Aqua dest.	Sigma-Aldrich Inc. (St. Louis, MO, USA)
Dehydroascorbic acid	100 µM	DMSO	Sigma-Aldrich Inc. (St. Louis, MO, USA)
Trolox	100 µM	Ethanol 100%	Sigma-Aldrich Inc. (St. Louis, MO, USA)

Table 7: Antioxidants

Antioxidant stock solutions (10 mM) were stored in aliquots at -80°C.

1.4. Antibodies

Target	Source	Dilution	Provider
phospho Akt Ser^{473}	rabbit, pc	1:2500	New England Biolabs (Beverly, MA, USA)
phospho Erk1/2 $Y^{202/204}$	rabbit, pc	1:1000	New England Biolabs (Beverly, MA, USA)
phospho p38 $Y^{180/182}$	rabbit, pc	1:1000	New England Biolabs (Beverly, MA, USA)
Src	rabbit, pc	1:1000	Cell Signaling (Danvers, MA, USA)
phospho Src Y^{418}	rabbit, pc	1:1000	Biosource (Camarillo, CA, USA)
phospho Src Y^{529}	rabbit, pc	1:1000	Biosource (Camarillo, CA, USA)
phospho STAT3 Y^{705}	rabbit, pc	1:1000	New England Biolabs (Beverly, MA, USA)
α-tubulin	mouse, mc	1:500	Santa Cruz (Santa Cruz, CA, USA)
phospho tyrosine (P-Tyr-100)	mouse, mc	1:1000	New England Biolabs (Beverly, MA, USA)

Table 8: Primary antibodies

Target	Source	Dilution	Provider
rabbit IgG	goat	1:2500	New England Biolabs (Beverly, MA, USA)
mouse IgG	goat	1:2500	Upstate (Charlottesville, VA, USA)

Table 9: Secondary antibodies, HRP-linked

The antibodies were diluted in TBS-T pH 8.0 as listed above. 5% BSA or 5% milk powder were added to TBS-T before dilution if recommended by the provider.

Target	Source	Concentration	Provider
v-Src	mouse, mc	1 mg/ml	Calbiochem (La Jolla, CA, USA)

Table 10: Immunoprecipitation antibody

The antibody was stored at 4°C until used for immunoprecipitation.

1.5. Buffers and solutions

Western blotting		**Reagents**
Lysis buffer (stock solution)	25 ml	HEPES 50 mM
	25 ml	NaCl 50 mM
	1.05 g	NaF 50 mM
	2.23 g	$Na_4P_2O_7$ x 10 H_2O 10 mM
	25 ml	EDTA
	91.95 mg	Na_3VO_4
	Reagents were dissolved in Aqua dest. (4°C) pH was adjusted to 7.5 solution was filled up to a final volume of 430 ml with Aqua dest.	
before use:	4.3 ml	Stock solution
	50 µl	PMSF 0.1 M
	202 µl	Complete™ 25x
	500 µl	Triton X-100 (10%)
CHAPS buffer pH 7,5	197.0 mg	Tris-HCl
	3.6 mg	EDTA
	4.7 mg	EGTA
	7.7 mg	DTT
	53.7 mg	Gluthation
	2.5 ml	Glycerol
	307.44 mg	CHAPS
	pH was adjusted to 7.5 solution was filled up to 25 ml with Aqua dest. and stored in 1.5 ml aliquots at -20°C	
Protease inhibitor cocktail	41.99 mg	NaF 200mM
	36.78 mg	Na_3VO_4 40 mM
	223.05 mg	$Na_4P_2O_7$ x 10 H_2O 100 mM
	Reagents were dissolved in 5ml Aqua dest. and stored in 50 µl aliquots at -20°C	

SDS – sample buffer, 3x	37.5 ml	Tris-HCl 0,5M pH 6.8
(stock solution)	6.0 g	SDS
	30.0 ml	Glycerol
	15.0 mg	Bromphenol blue
	ad 100.0 ml	Aqua dest.
before use:	85 %	Stock solution
	15%	β-mercaptoehanol
SDS 10%	5.0 g	SDS
	ad 50.0 ml	Aqua dest.
APS 10%	1.0 g	APS
	ad 10.0 ml	Aqua dest.
Complete™ 25x	one tablet	Complete™
	2.0 ml	Aqua dest.
PMSF 0.1M	52.26 mg	PMSF
	ad 3.0 ml	Aqua dest.
Resolving gel 10%	2.5 ml	PAA 30%
	1.875 ml	Tris-HCl 1.5M pH 8.8
	75 µl	SDS 10%
	3.05 ml	Aqua bidest.
	7.5 µl	TEMED
	37.5 µl	APS 10%
Stacking gel	640 µl	PAA 30%
	375 µl	Tris-HCl 1.25M pH 6.8
	37.5 µl	SDS 10%
	2.62 ml	Aqua bidest.
	7.5 µl	TEMED
	37.5 µl	APS 10%
Electrophoresis buffer, 10x	30 g	Tris-base
	144 g	Glycine
	10 g	SDS
	ad 1000 ml	Aqua bidest.
before use:	100 ml	10x Electrophoresis buffer
	ad 1000 ml	Aqua bidest.

Blotting buffer, 5x	15.17 g	Tris-base
	72.9 g	Glycine
	ad 1000 ml	Aqua bidest.
before use:	200 ml	5x Blotting buffer
	200 ml	Methanol bidest.
	ad 1000 ml	Aqua bidest.
Coomassie staining solution	0.4g	Coomassie brilliant blue R350
	200 ml	MeOH 40%
	200 ml	Acidic acid 20%
	Coomassie brilliant blue was dissolved in MeOH 40% and after filtration acidic acid 20% was added	
Coomassie destaining solution	500 ml	MeOH
	100 ml	Acidic acid 100%
	ad 1000 ml	Aqua dest.
Luminol (stock solution)	0.44 g	Luminol
	10 ml	DMSO
p-Coumaric acid (stock solution)	0.15 g	p-Coumaric acid
	10 ml	DMSO
ECL	4.5 ml	Aqua dest.
	500 µl	Tris-base 1M pH 8.5
	25µl	Luminol
	11 µl	p-Coumaric acid
	1.5 µl	H_2O_2 (30%)
TBS-T pH 8,0	3.0 g	Tris-base
	11.1 g	NaCl
	1 ml	Tween 20
	ad 1000 ml	Aqua dest.
	pH was adjusted to 8.0 with HCl conc.	

Table 11: Buffers and solutions

1.6. Cell culture

Cell culture: Reagents	Provider
Dulbecco's Modified Eagle Medium (DMEM), 4.5 g/l glucose, w/o L-glutamine, w/o phenolred	Lonza Group Ltd. (Basel, Switzerland)
Penicillin/streptomycin mixture (10.000 U/ml potassium penicilline/ 10.000 µg/ml streptomycin sulphate)	Lonza Group Ltd. (Basel, Switzerland)
L-glutamine 200 mM	Lonza Group Ltd. (Basel, Switzerland)
Calf serum	Lonza Group Ltd. (Basel, Switzerland)
Trypsin (1:250)	Invitrogen (Carlsbad, CA, USA)

Table 12: Cell culture reagents

Cell culture: Solutions		Reagents
PBS pH 7,4	36.0 g	NaCl
	7.4 g	Na_2HPO_4
	2.15 g	KH_2PO_4
	ad 5000 ml	Aqua dest.
Trypsin/EDTA in PBS	0.5 g	Trypsin
	0.2 g	EDTA
	1000 ml	PBS

Table 13: Cell culture solutions

Cell culture: Media		Reagents
Growth medium	500 ml	DMEM
	10%	Calf or foetal calf serum
	100 U/ml / 100 µg/ml	Penicillin / Streptomycin
	2 mM	L-glutamine
Starvation medium	500 ml	DMEM
	100 U/ml / 100 µg/ml	Penicillin / Streptomycin
	2 mM	L-glutamine

Freezing medium	1.1 ml	DMSO
	8.0 ml	Growth medium
	2.0 ml	Calf serum

Table 14: Cell culture media

1.7. Tyrosine kinase assay kit (chemiluminescent)

Components		Reagents
96-well plate (Streptavidin coated, 2 pieces)		
Substrate peptide (2 vials)	12.5 µg 250 µl	Poly-(Glu_4-Tyr)-peptide, biotin conjugate Sterile distilled water
Reference peptide	5 µg 50 µl	Poly-(Glu_4-phospho-Tyr)-peptide, biotin conjugate Sodium bicarbonate 0.1M
Tyrosine Kinase Reaction Buffer, 5x (1 vial á 5 ml)	100 mM 50 mM 5 mM 5 mM 1 mM	Tris-HCl pH 7.4 $MgCl_2$ $MnCl_2$ Dithiothreitol ATP
Sodium orthovanadate	500 µl	Na_3VO_4 50mM pH 10.0
TBS, 20x (1 vial á 50 ml)	1 M 3 M 2%	Tris NaCl Tween™-20
ELISA Blocking Buffer, 10x (1 vial á 25ml)	10% 0.05%	BSA in TBS pH 7.4 Kathon™
anti-p-Tyr HRP conjugate (recombinant, 4G10™)	25 µl 5 mg/ml 0.05%	IgG_{2bK}-HRP conjugate in PBS BSA Kathon™
LumiGLO™ Chemiluminescent substrate	10 ml	LumiGLO™ Reagent A
LumiGLO™ Chemiluminescent substrate	10 ml	LumiGLO™ Reagent B

Table 15: Tyrosine kinase assay kit components

The tyrosine kinase assay kit was provided by Upstate™, which is now part of Millipore™ (Billeria, MA, USA). Substrate peptide, reference peptide, tyrosine kinase reaction buffer and sodium orthovanadate were stored at -20°C, all the other components at 4°C.

1.8. Equipment

Name	Provider
Tecan GENios™Pro, Tecan Sunrise™	Tecan (Mannedorf, Switzerland)
LAS-3000™ Luminescent Image Analyzer	Fujifilm (Tokyo, Japan)
Light Microscope Olympus CKX 31	Olympus Europe GmbH (Hamburg, Germany)
Mini-PROTEAN™3 Cell	BIO-RAD Laboratories (Hercules, CA, USA)
Power Pac™ HC power supply	BIO-RAD Laboratories (Hercules, CA, USA)
Mini Trans-Blot™ Electrophoretic Transfer Cell	BIO-RAD Laboratories (Hercules, CA, USA)
Vi-Cell™ XR Cell Viability Analyzer	Beckman Coulter (Fullerton, CA, USA)
HERAsafe™ KS Workbench	Thermo Fisher Scientific Inc. (Waltham, CA, USA)
HERAcell™ 150 Incubator	Thermo Fisher Scientific Inc. (Waltham, CA, USA)
Heraeus™ Multifuge™ 1 S-R Centrifuge	Thermo Fisher Scientific Inc. (Waltham, CA, USA)
Heraeus™ Fresco™ Centrifuge	Thermo Fisher Scientific Inc. (Waltham, CA, USA)
Galaxy Mini Microcentrifuge	VWR International Inc. (West Chester, PA, USA)
Vortex Shaker	VWR International Inc. (West Chester, PA, USA)
RCT basic Magnetic Stirrer	IKA™ Laboratory equipment (Staufen, Germany)
Vibrax VXR basic Shaker	IKA™ Laboratory equipment (Staufen, Germany)
Heraeus™ B15 Incubator	Thermo Fisher Scientific Inc. (Waltham, CA, USA)

Table 16: Equipment

1.9. Software

Name	Provider
AIDA™ (Advanced Image Data Analyzer) Version 4.06	Raytest GmbH (Straubenhardt, Germany)
GraphPad PRISM™ Version 4.03	GraphPad Software Inc. (San Diego, CA, USA)
Image Reader LAS-3000™ Version 2.0	Fujifilm (Tokyo, Japan)
Vi-Cell™ XR 2.03	Beckmann Coulter (Fullerton, CA, USA)

Table 17: Software

1.10. Consumables

Name	Provider
Immun-Blot™ PVDF Membrane (0.2 µm)	BIO-RAD Laboratories (Hercules, CA, USA)
Precision Plus Protein™ Standard	BIO-RAD Laboratories (Hercules, CA, USA)
Gel Blotting Paper	Whatman plc (Kent, UK)
Serological Pipettes (1ml, 2ml, 5ml, 10ml, 25ml)	Sarstedt GmbH (Nümbrecht, Germany)
Tissue Culture Flask 75cm^2	Sarstedt GmbH (Nümbrecht, Germany)
Tissue Culture Dishes (60mm, 100mm)	Greiner bio-one (Frickenhausen, Germany)
96-well Microplates	Greiner bio-one (Frickenhausen, Germany)
PP – Test tubes (15ml, 50 ml)	Greiner bio-one (Frickenhausen, Germany)
Cell scraper	Greiner bio-one (Frickenhausen, Germany)
Protein A/G Agarose Plus	Santa Cruz (Santa Cruz, CA, USA)

Table 18: Consumables

2. Methods

2.1. Cell culture techniques

2.1.1. Cell lines

Most of our cell-based experiments were performed with vascular smooth muscle cells between passage 7 and 14, isolated from thoracic aortas of male Sprague-Dawley rats. As part of the troubleshooting procedure a single tyrosine kinase assay was additionally performed with mouse endothelial fibroblasts and MCF-7 breast cancer cells. All kind of cell culture work was performed in the same way for all three different cell lines and is described on the basis of VSMCs.

2.1.2. Thawing cells

Fresh cells at passage 7 were stored in aliquots of 1.5 million in liquid nitrogen. The first step, when preparing the cells for further cultivation, was to thaw one of the aliquots. Therefore one of the cryovials was removed from the nitrogen tank and thawed in a water bath at 37°C. Under the laminar hood the cell suspension was immediately transferred into a prepared falcon with 9 ml growth medium. After 10 minutes of centrifugation at 1000 rpm the supernatant fraction, containing growth medium and freezing medium, was disposed and 10 ml of fresh growth medium were added to the remaining cell pellet. By a brief vortex pulse the cell pellet was resuspended and the cell suspension was transferred into a 75 cm^2 tissue culture flask, which was placed in an incubator for further cultivation.

2.1.3. Cultivation

To assure optimal cell growth VSMCs were cultured at 37°C and 5% CO_2 with daily medium change, whereas the cells showed a doubling time of 24 hours. If a daily medium change was not possible, additional 10 ml of growth medium were added for each cultivation day. The cells were kept under these conditions until they grew at near confluence, which made passaging once or twice a week necessary. The first step when passaging the cells was to discard the growth medium in which the cells were cultivated from the culture flask. Afterwards the cells were washed

with 10 ml of PBS to remove the last remaining traces of calf serum, which is part of the growth medium. Calf serum would inhibit the protease trypsin, which is used to detach the cells from the surface of the culture flask in the next step. Therefore 3 ml of trypsin/EDTA were added to the cells, which were stored in the incubator for a maximum of three minutes. A light microscope was used to verify that all cells were detached from the surface by the trypsin/EDTA treatment. Remaining cell aggregates were resolved by mechanic force. To inhibit trypsin from lysing the cells 7 ml of growth medium were added and the suspension, containing cells, growth medium and trypsin was transferred into a prepared falcon. The culture flask was rinsed with additional 5 ml of growth medium to remove the last remaining cells, which were also moved into the falcon. After centrifugation for 4 minutes at 1400 rpm the supernatant fraction was removed, 10 ml of fresh growth medium were added to the falcon and the cells were resuspended by a vortex pulse.
To determine the total amount of viable cells received from the harvest, 500 µl of the suspension were transferred into the ViCell™ XR Cell Viability Analyzer. The cells were counted by the trypan-blue dye exclusion method, which is based on the fact that trypan blue is able to penetrate through the membrane of dead cells but not through those of viable cells.

After the count, exact numbers of cells were seeded into new 75 cm^2 culture flasks for further cultivation. For experiments, cells were seeded in 60 or 100 mm dishes and stimulated with 20 ng/ml PDGF-BB, when they reached 70 – 90 % confluence. To allow a maximum response to growth factor stimulation, cells were incubated with starvation medium 24 hours prior to stimulation.

2.2. Western blot

2.2.1. Sample preparation

Cells were seeded in 60 mm dishes and cultivated at 37°C and 5 % CO_2 with growth medium until they reached 70 – 80 % confluence. 24 hours in advance of the stimulation the cells were incubated with starvation medium and thus because of the absence of serum, kept quiescent. After an additional hour of incubation with fresh starvation medium, I3MO and dasatinib were added in the appropriate concentrations and allowed to act on the cells for 30 minutes. If antioxidants were used, the preincubation with the reagents was performed for one hour instead of 30 minutes. DMSO (1 %) which was used as solvent for dasatinib and I3MO was added to the control cells. In case of the antioxidants the respective solvents used (distilled water, DMSO and ethanol 100 %) were used as controls. As soon as the preincubation procedure was finished, the cells were stimulated with 20 ng/ml PDGF-BB for the desired time point. After successful PDGF-BB stimulation, medium, growth factor and reagents were removed from the dishes by using a vacuum pump and the cells were washed twice with ice-cold PBS. On ice, 200 µl lysis buffer were added to each dish and the cells were lysed for 30 minutes at 4°C. To receive the cell lysates, cells were scrapped of the dishes and transferred into pre-chilled tubes. By centrifugation for 10 minutes at 4°C with 13.000 g the lysates were cleared from cell components. 10 µl of each sample were kept aside to perform a Bradford protein quantification assay later on. Remaining lysates were separated from the cell components by transferring them into fresh pre-chilled tubes, where they were diluted with 3x SDS sample buffer (including 15 % ß-mercaptoethanol) and afterwards boiled for 5 minutes at 95°C. The finished samples were stored at -20°C until the SDS – PAGE was performed.

2.2.2. Bradford protein quantification

To determine the exact amount of protein contained in each sample a Bradford assay was performed. The basic mechanism of the assay is based on a shift of the absorption maximum of Coomassie Brilliant Blue G-250 in acidic environment from 465 to 595 nm, when interacting with basic or aromatic side chains of proteins.

Therefore the 10 µl separated from each lysate were diluted in 90 µl distilled water and triplicates of 10 µl from each diluted sample were transferred into a 96-well plate. A standard curve was prepared by diluting increasing concentrations of BSA (50 – 500 ng/ml) in distilled water, which were afterwards transferred in triplicate into the
96-well plate. Finally 190 µl Bradford solution was added to each occupied well and the plate was incubated for 5 minutes at room temperature. The absorbance measurement was performed at 595 nm with a Tecan Sunrise™ microplate reader.

2.2.3. SDS-PAGE

To separate the different proteins contained in each sample and to enable a specific detection of single proteins of interest a sodium dodecylsulfate polyacrylamide gel electrophoresis (SDS – PAGE) was performed.
The previous treatment with an excess of SDS, an anionic detergent which binds to hydrophobic parts of the protein, caused the loss of secondary protein structures by breaking hydrogen bonds. Tertiary structures, such as disulfide bonds, were cracked by reducing agents like ß-mercaptoethanol. As an additional effect induced by SDS the protein charges were covered with the constant negative charge of SDS, leaving a constant molecular weight/charge relation. Therefore the only parameter left for separation via electrophoresis is the different molecular weight of the proteins.

Before the electrophoresis was performed, the gels had to be prepared. Usually two gels were prepared at the same time caused by the ability of running two gels at the same time in one chamber. First of all a spacer plate and a short glas plate were mounted together by a casting frame to form the gel cassette assembly. Fixed in a casting stand, the gel cassette assembly was filled with distilled water to check if both plates are flush at the bottom. In the meantime the resolving gel was prepared and transferred into the gel cassette assembly if both plates proved to be flush. The resolving gel was covered with a layer of isopropanol to remove bubbles from the surface. After 45 (- 60) minutes of polymerization the isopropanol was removed and remaining traces were removed with a filter paper. The stacking gel was prepared and the solution was placed above the hardened resolving gel. A 10-well comb was inserted and the gel was allowed to polymerize for one hour. The hardened gel

cassette sandwich was transferred into the electrode assembly, both were fixed inside the clamping frame and the inner chamber was moved into the tank of the Mini-PROTEAN™ 3 cell system, after filling it with ~125 ml electrophoresis buffer. After removing the comb, the wells were loaded with samples and Precision Plus™ protein standard was placed in the external left well. 200 ml of electrophoresis buffer were filled into the tank and electrophoresis was first performed for 21 minutes at 110 V to stack the proteins and 36 minutes at 200 V to resolve them.

2.2.4. Western blotting

When separated by SDS – PAGE, the proteins had to be transferred to a PVDF membrane to allow immunodetection. The transfer of the proteins was performed via the tank blotting technique using a Mini Trans-Blot™ electrophoretic transfer cell. To prepare the membrane, it was first inserted in distilled methanol and afterwards in blotting buffer. In the meantime the gel cassette sandwich was prepared, by placing the cassette in an adequate vessel, filled with blotting buffer. A fiber pad was placed on the bottom side of the cassette and covered with a sheet of filter paper, on which the gel and afterwards the membrane were placed. To complete the sandwich, another sheet of filter paper and a second fiber pad were placed above the membrane. The cassette was locked and placed in the electrode module, which was fixed in the tank. A cooling unit was added and the tank was completely filled with blotting buffer. After adding a magnetic stir bar to maintain the temperature constant throughout the buffer, the transfer cell was connected to the power supply and the blot ran for 90 minutes at 100 V.

2.2.5. Staining of gels

To control equal protein loading and blotting, gels were stained with Coomassie blue staining solution after western blotting. Coomassie blue penetrates into the membrane and remains permanently bound to the proteins after 20 minutes of staining at room temperature. When washing the gels several times with Coomassie destaining solution the proteins appear as blue bonds on the gel.

2.2.6. Detection

Immunodetection is based on a two-stage antigen-antibody reaction. A primary antibody, which specifically binds the protein of interest, is incubated with the membrane. Before the secondary antibody is added, washing steps are performed to remove unspecific bound antibody. The horse reddish peroxidase-conjugated (HRP) secondary antibody is aimed against specific regions of the primary antibody, favoured the Fc-region, and binds them during incubation. Addition of a chemiluminescent substrate solution (ECL) allows the enzyme horse reddish peroxidise (HRP) to create a light signal, which can be used for detection of the protein bands of interest by using a luminescent image analyzer.
After the transfer, the membranes were blocked by incubating them with 5 % milk powder at room temperature for one hour on a shaking platform to avoid unspecific binding of the antibodies. To remove last traces of the milk powder three washing steps, each taking 10 minutes, were performed with TBS-T and the membranes were incubated with specific primary antibodies at 4°C over night. The secondary, horse reddish peroxidase-labelled antibody was added after three more washing steps. Depending on how many times the secondary antibody has been used before, the membrane was incubated between 45 minutes and 3 hours at room temperature. Three more washing steps with TBS-T were performed, before ECL-solution was added and the protein bands were detected with a LAS-3000™ luminescent image analyzer. AIDA™ software was used for quantification.

2.3. *In vitro* tyrosine kinase assay

The non-radioactive tyrosine kinase assay was performed to detect possible inhibitory effects of indirubin-3'-monoxime on the phosphotransferase activity of Src-kinase and to determine the scale of the inhibition. Due to the fact that both immunoprecipitated Src from cell lysates and purified recombinant Src were used for the assay, two different protocols were applicable.

2.3.1. Principle

The assay itself is based on a two-step peptide phosphorylation detection. A biotinylated poly-(Glu_4-Tyr)-peptide ('substrate peptide') is bound to a streptavidin-coated 96-well microplate, where it is captured due to the very strong biotin-streptavidin interactions. During incubation together with a tyrosine kinase in the presence of ATP and a Mn^{2+}/Mg^{2+} co-factor cocktail, the kinase transfers phosphate residues from ATP to the tyrosine residues of the substrate peptide. Increasing concentrations of a poly-(Glu_4-phospho-Tyr)-peptide ('reference peptide') serve as positive control for the assay. The phosphorylated tyrosine residues are detected via ELISA, after addition of a monoclonal anti-phosphotyrosine-HRP antibody conjugate. After incubation with a chemiluminescence substrate the detection can be accomplished with a Tecan GENios™ Pro microplate reader.

2.3.2. Procedure for enzymes in immune complexes

2.3.2.1. Sample preparation

For the tyrosine kinase assay cells were seeded out in 100 mm dishes and cultivated until grown to 80 – 90 % confluence. After treating them 24 hours with starvation medium the cells were preincubated for one hour with fresh starvation medium and, prior to stimulation, 30 minutes with dasatinb or indirubin-3'-monoxime. DMSO (1%) was used as control. The cells were stimulated with 20 ng/ml PDGF-BB or calf serum for the desired time point to induce signal transduction. Supernatant medium was removed after stimulation, the cells were washed twice with ice-cold PBS and 200 µl lysis buffer were added to each dish. On ice, the dishes were kept

30 minutes at 4 °C to lyse. To receive the lysates, the cells were scraped of the dishes and transferred into pre-chilled tubes. These tubes were centrifuged for 10 minutes at 4°C with 13,000 g to clear the lysates from cellular components. The cleared lysates were transferred into fresh tubes and 10 µl from each sample were kept aside for the Bradford protein quantification.

2.3.2.2. Sample preparation with CHAPS buffer

As part of our troubleshooting procedure we were forced to modify the protocol for sample preparation to exclude the possibility that the assay might not work in VSMC. We therefore decided to perform the assay with other cell lines, such as MEF (mouse embryonic fibroblasts) and MCF-7 breast cancer cells. We also decided to treat each of the cell lines with a different lysis buffer instead of the common used one. CHAPS buffer was selected because of its ability to even gain access to membrane proteins, an important fact due to the capability of c-Src to anchor in cell membranes with its myristoylated N-terminal domain.
The different lysis buffer required a slightly different way of sample preparation. Before treating the cells with CHAPS buffer, 40 µl Complete and 50 µl protease inhibitor cocktail were added per mililiter buffer needed. After adding the buffer to the previously with 20 ng/ml PDGF-BB stimulated cells, the cells were scraped of immediately, transferred into pre-chilled tubes and incubated for 15 minutes on ice. The tubes were placed in an ultrasonic bath for one minute and afterwards centrifugated for 10 minutes at 4°C with 13,000 g. The last steps of the sample preparation were performed similarly to ‘normal’ lysis buffer.

2.3.2.3. Protein quantification

A Bradford assay was performed to determine which volume of each sample was necessary to achieve a protein concentration of 550 µg protein. After transferring the calculated volume into fresh tubes, the samples were filled up with lysis buffer to a final volume of 550 µl.

2.3.2.4. Immunoprecipitation

To clear our samples from proteins causing unspecific interactions, which would lead to falsified results in our tyrosine kinase assay, an immunopreciptiation was performed.

After pre-clearing the samples from unspecific binding proteins by adding protein A/G agarose beads (preclearing), an antibody, with a Fc-region from mammalian Ig, against the protein of interest was added. Based on an antigen-antibody reaction the antibody binds the protein and forms a soluble antigen-antibody-complex. Protein A and G bind the Fc-region of most mammalian Ig very specific. By adding protein A/G agarose beads again, the former soluble complex gets insoluble and can be separated by centrifugation from the other proteins in the sample. After a few washing steps we received a purified lysate with an increased concentration of our protein of interest.

Usually the preclearing and addition of the antibody were performed one day in advance of the actual tyrosine kinase assay. Only collecting of the immune complexes was done on the same day as the assay.

To preclear our samples, 25 µl of protein A/G agarose beads were added to our samples and rotated end-over-end for one hour at 4°C. The beads, now containing unspecific binding proteins, were collected by centrifuging the samples for 5 minutes with 13,000 g. The supernatant fraction was separated from the pellet by transferring it into fresh tubes, per 500 µl of lysate12.5 µl of an anti-v-Src mouse antibody were added and the samples were mixed over night at 4°C. To collect the immune complexes, 12.5 µl protein A/G agarose beads were added. After one hour of rotating end-over-end, the antigen-antibody-bead complexes were collected by centrifugation (5 minutes, 13,000g).

2.3.2.5. Well rehydration

The well rehydration was usually done on the same day as the immunoprecipitation and therefore one day in advance of the actual assay procedure. A sufficient amount of 1x TBS-T and 1x ELISA Blocking Buffer for the number of wells needed had to be prepared before starting the rehydration. Therefore 20x TBS-T stock solution was

diluted 1:20 with sterile distilled water and 10x ELISA stock solution 1:10 with 1x TBS-T.
100 µl of 1x TBS-T were added to each well and incubated for 15 minutes at room temperature. After removing 1x TBS-T from the wells 300 µl of 1x ELISA Blocking Buffer were added to each well and incubated over night.

2.3.2.6. *In vitro* kinase assay

Prior to the assay sufficient 1x TBS-T and lysis buffer for the whole experiment had to be prepared by diluting 20x TBS-T stock solution with sterile distilled water. Afterwards the final steps of the immunoprecipitation were performed. 12.5 µl of protein A/G agarose beads were added to the samples and rotated one hour end-over-end to collect the Src-antibody-bead complexes. While the samples were rotating, Tyrosine Kinase Reaction Buffer, Sodium orthovanadate and the substrate peptide (12.5 µg in 250 µl) were thawed on ice. Sodium orthovanadate and Tyrosine Kinase Reaction Buffer were part of the 'Master Mix', a reaction mix to enable an optimal environment for phosphorylation of the substrate peptide by Src-kinase. As soon as all reagents were ready. 50 µl Master Mix for each experimental well were prepared in separate tubes and stored on ice until the precipitated Src was ready for further processing.

Reagent	Amount
Tyrosine Kinase Reaction Buffer (5x Stock Solution)	10 µl
Sodium Orthovanadate 50 mM	1 µl
Poly-(Glu_4-Tyr)-Peptide (12.5 µg/ 250 ml)	5 µl
Sterile Distilled Water	34 µl

Table 19: Preparation of the Tyrosine Kinase Assay Master Mix
After mixing distilled water and Tyrosine Kinase Reaction Buffer the substrate peptide was added. The phosphatase inhibitor Sodium Orthovanadate was added last because of its small amount.

After rotating for one hour the Src-antibody-bead complexes were collected by centrifugation and the supernatant fraction was removed. The remaining beads were washed five times with 200 µl lysis buffer and finally with 100 µl 1x tyrosine kinase reaction buffer (TKRB). As much buffer as possible was removed from the beads

and Master Mix was added to precipitated Src. The tubes with Src-Substrate-Mix were incubated for 10 minutes under agitation at 37°C. In the meantime Reference Solution and Substrate Solution were prepared by diluting Reference Peptide stock solution 1:100 with 1x TBS-T and Substrate Peptide stock solution 1:50 with 1x TBS-T to a final concentration of 1 µg/ml. Reference Series was prepared by mixing increasing amounts of Reference Solution with Substrate Solution to a final volume of 100 µl.

Reference Series	Reference Peptide (ng)	Volume Reference Solution (µl)	Volume Substrate Solution (µl)
Ref. 0	0	0	100
Ref. 1	1	1	99
Ref. 2.5	2.5	2.5	97.5
Ref. 5	5	5	95
Ref. 10	10	10	90

Table 20: Preparation of Reference Series
Reference Solution and Substrate Solution were prepared by diluting the corresponding stock solutions to a final concentration of 1µg/ml with 1x TBS-T. After producing Substrate Solution in tubes, Reference Solution was added and the tubes were stored on ice until used.

The reaction between kinase and substrate was terminated by cooking the samples for 5 minutes at 95°C. Blocking Buffer was removed from the 96-well microplate and the wells were rinsed with 300 µl 1x TBS-T. After centrifugation, Src-Substrate-Mix and Reference Series were transferred into individual wells. The well plate was covered with a sealing film and incubated for 1 hour at 37°C. To remove last traces from the Src-Substrate-Mix the wells were rinsed twice with 300 µl 1x TBS-T after incubation. Four more washing steps with 300 µl 1x TBS-T were performed with 10 minutes incubation at room temperature and agitation between the buffer changes.

2.3.2.7. Phosphotyrosine detection

During the last incubation period the anti-phosphotyrosine-HRP antibody conjugate was prepared by diluting the antibody stock solution 1:250,000 with prior prepared 1x ELISA Blocking Buffer. The anti-p-Tyr-HRP conjugate was removed after 30

minutes of incubation at room temperature. After rinsing the wells once with 300 µl 1x TBS-T five more washes with 1x TBS-T were performed, incubating the microplate 2 minutes at room temperature with agitation between the buffer changes. During the last wash sufficient amount of the LumiGLO™ chemiluminescent HRP substrate was prepared by mixing LumiGLO™ Reagent A and B 1:1. The plate was once more washed with 300 µl distilled water to remove last traces of TBS-T. TBS-T has to be removed completely because of the contained Tween-20, which is able to interact with HRP-activity. After removing the last traces of liquids which could alter the luminescence signal, 75 µl of the LumiGLO™ Chemiluminescent HRP Substrate were added to each well. The luminescence was measured with a Tecan GENios™ Pro microplate reader, 10 and 15 minutes after the addition of LumiGLO™. The results of the measurements were declared in relative light units (RLU).

2.3.3. Procedure for enzymes in solution

Because of the abolition of sample preparation and immunoprecipitation when using purified recombinant enzymes in solution to perform the assay the whole procedure, including well rehydration, was performed on one day.

2.3.3.1. Well rehydration

As well as for immobilized enzymes, sufficient 1x TBS-T had to be prepared in advance of the assay. While incubating the 96-well microplate for 15 minutes at room temperature with 100 µl 1x TBS-T in each well required, Kinase Substrate Solution and Kinase Reference Solution were prepared by diluting prior thawed Kinase Substrate Peptide stock solution 1:50 and Kinase Reference Peptide stock solution 1:100 with 1x TBS-T to a final concentration of 1 µg/ml. A Reference Series was prepared, by mixing Substrate Solution and Reference Solution as stated under point 2.3.2.6. The solutions and the Reference Series were stored on ice until used.

2.3.3.2. Binding peptides to the plate

After removing the 1x TBS-T from the wells 100 µl Kinase Substrate Solution and the Reference Series were added to individual wells. The plate was covered with a sealing film and incubated for one hour at 37°C. Finally the wells were rinsed once

with 300 µl 1x TBS-T after incubation to remove unbound peptide and the plate was incubated another hour at 37°C with 300 µl 1x ELISA Blocking Buffer in each well.

2.3.3.3. *In vitro* kinase assay

To prepare 50 µl Master Mix for each experimental well 5x Tyrosine Kinase Reaction Buffer, Sodium orthovanadate, I3MO, DMSO and recombinant c-Src were thawed up on ice while incubating the microplate. I3MO 0.3 µM was used as a Src-kinase inhibitor, while DMSO (1%) served as control. The preparation of the Master Mix was timed so that I3MO was able to interact with c-Src for 15 minutes.

Reagent	Amount
Tyrosine Kinase Reaction Buffer (5x stock solution)	10 µl
Sodium orthovanadate 50 mM	1 µl
Purified recombinant c-Src	0.1 – 5 µl
I3MO 0.3 mM or DMSO 1%	0.5 µl
Aqua dest.	ad 50 µl

Table 21: Preparation of Master Mix for enzymes in solution
Distilled water and 5x TKRB were produced, followed by Sodium orthovanadate and recombinant Src. I3MO addition was timed, so that I3MO could interact with c-Src for 15 minutes until further processing. 1% DMSO was used as control.

Blocking buffer was removed and the wells were rinsed once with 300 µl 1x TBS-T. After adding 100 µl 1x TBS-T to each reference well and 50 µl Master Mix to each experimental well, the plate was incubated for 10 minutes at 37°C. Before proceeding to phosphotyrosine detection, all wells were rinsed once with 300 µl 1x TBS-T. 4 additional washes were performed, incubating the plate 2 minutes at room temperature with agitation between the buffer changes.

2.3.3.4. Phosphotyrosine detection

The recombinant anti-p-Tyr-HRP antibody conjugate was prepared for detection by diluting the antibody stock solution 1:250.000 with 1x ELISA Blocking Buffer, prepared in advance. After incubating with the antibody conjugate 30 minutes at room temperature the wells were rinsed once and washed four times with 300 µl 1x

TBS-T. During the washing steps the plate was incubated 2 minutes at room temperature with agitation between the buffer changes. LumiGLO™ Chemiluminescent HRP Substrate was prepared during the last washing step by mixing its reagents A and B 1:1. 75 µl of the chemiluminescent substrate were added to each well after rinsing them one last time with 300 µl distilled water. The luminescence was detected 10 and 15 minutes after the addition of the LumiGLO™ Chemiluminescent Substrate with a Tecan GENios™ Pro microplate reader and declared in relative light units (RLU).

2.4. Statistics

Statistical analysis of experimental data was performed with GraphPad PRISM™ software by using one-way ANOVA with subsequent Dunnett multiple comparison test. In case of time courses, I3MO treated and untreated samples at different time points were compared via one-tailed paired t-test. Results are shown as means with standard error of the mean (SEM), whereas significance was considered at p values <0.05. Each experiment was performed at least three times.

D RESULTS

D RESULTS

1. Effects of I3MO on Akt and Erk1/2 kinases

PDGF is one of the most important mitogens for VSMCs and other cell types of mesenchymal origin leading to cell proliferation and migration. Beside others, the MAPK- and PI3K-pathway are crucially involved in PDGF-induced signalling.[17,19]
To verify the effects of I3MO on these two pathways we selected representative signalling molecules and determined their activity in the presence and absence of I3MO. Akt kinase was selected to represent the PI3K-pathway, while Erk1/2 kinases were chosen from the MAPK-pathway.
Based on the fact that kinase activity often correlates with their phosphorylation status, we measured changes at critical phosphorylation sites of the kinases in VSMCs experiencing I3MO treatment in advance of PDGF-BB stimulation compared to VSMCs not receiving I3MO treatment.
These initial experiments were performed to reproduce the results from previous studies, required for the comparison of future experimental results concerning cellular effects of I3MO on VSMC after PDGF-BB stimulation.[36]

For our time courses 24 h serum-starved VSMCs received 30 minutes of I3MO pretreatment and were afterwards stimulated up to 10 minutes with PDGF-BB. VSMCs only treated with 1 % DMSO, serving as vehicle, were used as comparison to define the effects of I3MO at a concentration of 3 µM on PDGF-induced signalling cascades.

After replicating each experiment three times, the received results illustrated in Fig. 8 showed only marginal differences in Akt phosphorylation between I3MO-treated and untreated cells at all measured time periods. The same was observed for Erk1/2 kinases, although I3MO caused a decreased phosphorylation of both Erk kinases at 2 minutes of PDGF stimulation. The effect was classified irrelevant because of the return to physiological phosphorylation levels at 5 minutes after PDGF stimulation, where it was kept maintained until the final time point of the experiments.

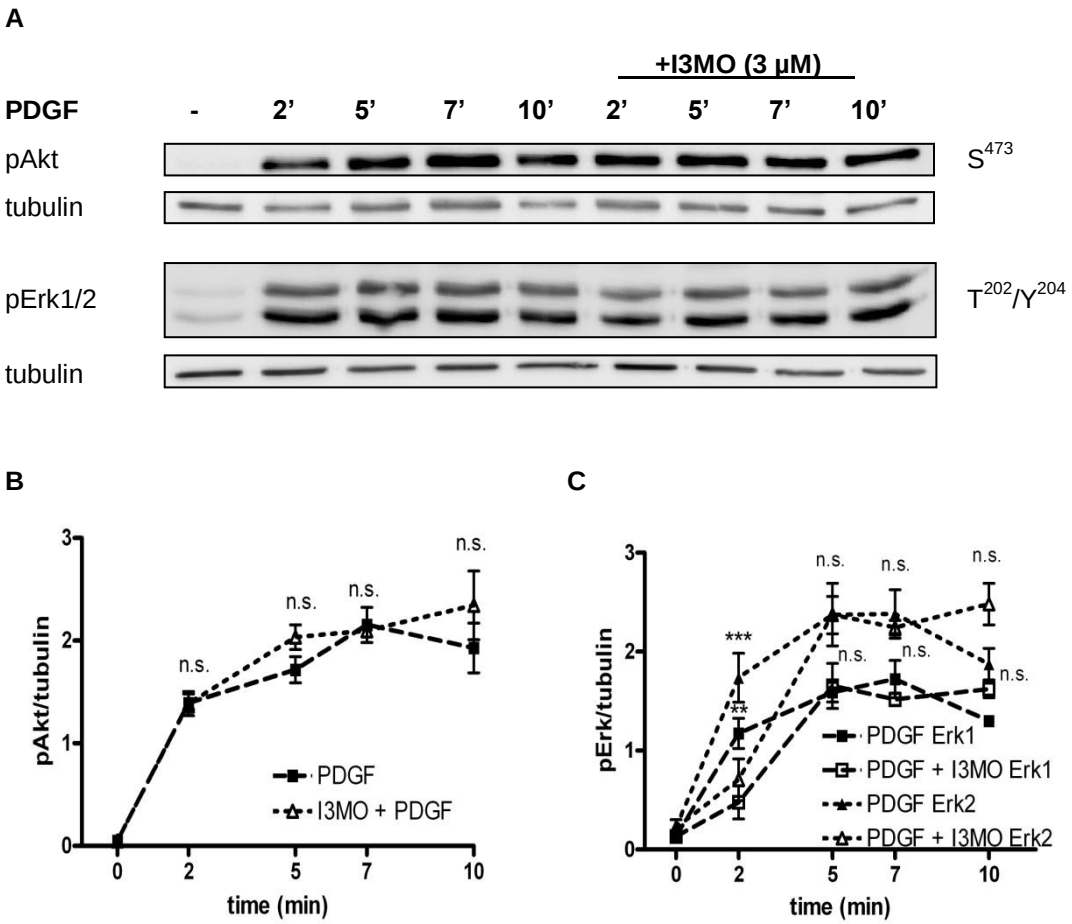

Figure 8: I3MO does not affect phosphorylation/activation of Akt and Erk1/2 kinases

24 hour serum-starved VSMC were stimulated with 20 ng/ml PDGF-BB for the declared time periods after treatment for 30 minutes with I3MO 3 µM or DMSO 1 %, serving as vehicle. Lysates were prepared as stated in the Materials and Methods section. For immunoblotting specific antibodies against phospho-Akt (S^{473}) and phospho-Erk1/2 (T^{202}/Y^{204}) were used; tubulin served as loading control. Experiments were performed three times. Shown are representative western blots, chosen out of the performed experiments (A), and averaged, time dependent changes in phosphorylation status in the presence and absence of I3MO 3 µM of Akt (B) and Erk1/2 (C). ***p<0.001, n.s. (not significant) p>0.05 (t-test).

2. Effect of I3MO on c-Src activation via Y^{418} and Y^{529}

c-Src kinase is known today as an important mediator of PDGF-induced signalling. The kinase binds to phosphorylated PDGFR which leads to increased kinase activity and phosphorylation of Src target proteins.
The main mechanism regulating the kinase activity is based on phosphorylation and dephosphorylation of two major involved tyrosine residues, Y^{418} as upregulating residue and Y^{529} as downregulating residue.
Increased phosphorylation at Y^{418} causes steric interactions, leading to dislocation of Y^{418} from the kinase substrate binding pocket and better accessibility for potential phosphorylation substrates. In contrast, phosphorylation of Y^{529} causes augmented interactions of the phosphorylated tyrosine residue with the SH2 domain of the kinase, transferring it into the inactive conformation.[5]

Time courses were performed to expose a potential effect of I3MO on c-Src kinase activation in PDGF-stimulated VSMCs by stimulating serum-starved cells up to 10 minutes with 20 ng/ml PDGF-BB following a 30 minutes treatment with I3MO (3 µM).To determine a possible effect, we monitored the phosphorylation status of the above mentioned tyrosine residues, mainly responsible for c-Src activation, respectively inactivation.

As shown in Fig. 9, Y^{418} seems to remain unaffected by I3MO treatment, whereas the tyrosine residue Y^{529} showed a slight dephosphorylation after 2 minutes of PDGF stimulation. Due to its return to physiologic phosphorylation levels after 5 minutes, we accounted this dephosphorylation as deficient to achieve any notable effect on c-Src activation.

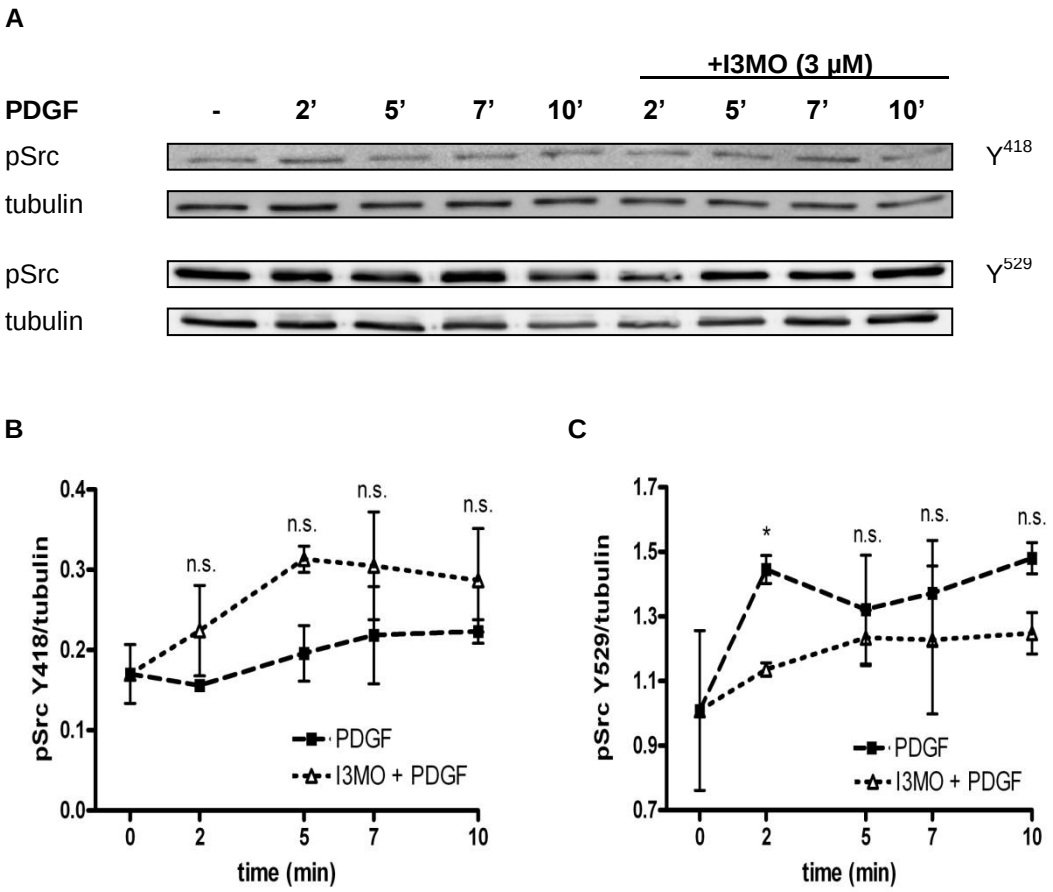

Figure 9: I3MO does not affect phosphorylation of Y^{418} or Y^{529}

After 30 minutes preincubation with I3MO 3 µM or DMSO 1 % (vehicle) serum-starved VSMC were stimulated with 20 ng/ml PDGF-BB for up to 10 minutes. The received lysates were prepared as described in the Material and Method section. Immunoblotting was performed with specific antibodies against phospho-Src (Y^{418} and Y^{529}), tubulin was used as loading control. After 3 replications of the experiments, data were analysed via 2D – densitometry. Shown are representative western blots (A) and a comparison of phosphorylation status of Y^{418} (B) and Y^{529} (C) at the indicated time points in the presence or absence of I3MO 3 µM. * $p<0.05$, n.s. (not significant) $p>0.05$ (t-test).

3. Comparison of I3MO with dasatinib, a synthetic Src-/Bcr-Abl kinase inhibitor

For the purpose of knowing more about the molecular mechanism of I3MO as a potential Src-kinase inhibitor, we compared its effect on PDGF-stimulated VSMCs with dasatinib, a synthetic Src-/Bcr-Abl-kinase inhibitor, which is used as therapeutic agent for the treatment of imatinib-resistant chronic myeloic leukemia as well as an experimental Src-kinase inhibitor.[31]

Serum-starved VSMCs were stimulated with PDGF-BB for 2 and 10 minutes, respectively, after receiving 30 minutes of treatment with I3MO, dasatinib or DMSO (1 %), serving as vehicle; unstimulated cells were used as controls. After performing each experiment three times, results were obtained by densitometric analysis of western blots performed with the prepared cell lysates.

As potential targets for both inhibitors we checked the overall autophosphorylation of the PDGF-R, c-Src kinase activity (via phosphorylation of Y^{418} and Y^{529}), activation of the Src downstream substrate STAT3 (via phosphorylation of Y^{705}) and total Src protein level.

Autophosphorylation of the PDGF-R is the initial step in creating necessary binding sites for SH2 domain-containing adaptor proteins or downstream signalling molecules. A particular binding site is created by phosphorylation of $Y^{579/581}$, necessary for the association of SFKs.[5,18] Treatment with dasatinib causes abolition of PDGF-induced receptor autophosphorylation, whereas I3MO shows a slighter reduction of the overall receptor phosphorylation as dasatinib.
As depicted in Fig. 10 reduction of PDGF-R autophosphorylation was clearly detectable for I3MO as well as for dasatinib in all three performed experiments. Nevertheless, statistical evaluation of the received results surprisingly showed that the effect was not significant for both I3MO and dasatinib, which, however, may be caused by large interexperimental variance or randomisation to tubulin.

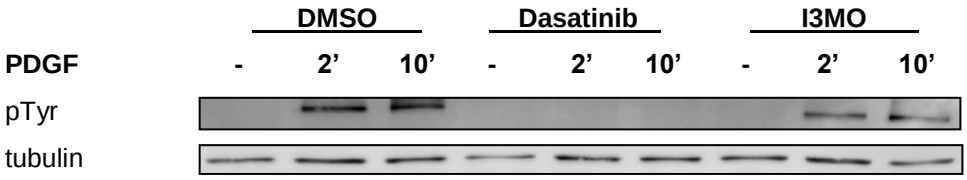

Figure 10: Dasatinib and I3MO diminish overall PDGF-R phosphorylation

VSMC kept abstinent from serum for 24 hours were stimulated with 20 ng/ml PDGF-BB, after preincubating them 30 minutes with I3MO 3 µM, dasatinib 100 nM and DMSO 1 %. Lysates were prepared as listed in the Material and Method section. Immunoblotting was performed with an antibody against phospho-tyrosine, tubulin was used as loading control.

A representative western blot, selected out of the three performed experiments is shown.

As mentioned before, one of the downstream signalling molecules activated after PDGF-R autophosphorylation is c-Src, a non receptor tyrosine kinase. Binding to the activated PDGF-R causes disruption of interactions keeping the kinase in its inactive state and leads to activation of the c-Src/STAT3/c-myc signalling cascade.[19,30] Maintenance of Y^{529} phosphorylation or suppression of Y^{418} phosphorylation represent two possible mechanisms to inhibit PDGF-induced c-Src activation. We compared the phosphorylation status of Y^{529} and Y^{418} in PDGF-stimulated VSMCs pre-treated with I3MO or dasatinib. While phosphorylation of both tyrosine residues remained unaffected by I3MO treatment, dasatinib-treated VSMCs showed significant dephosphorylation of Y^{529}. Activity upregulating Y^{418} was, however, not affected by dasatinib.

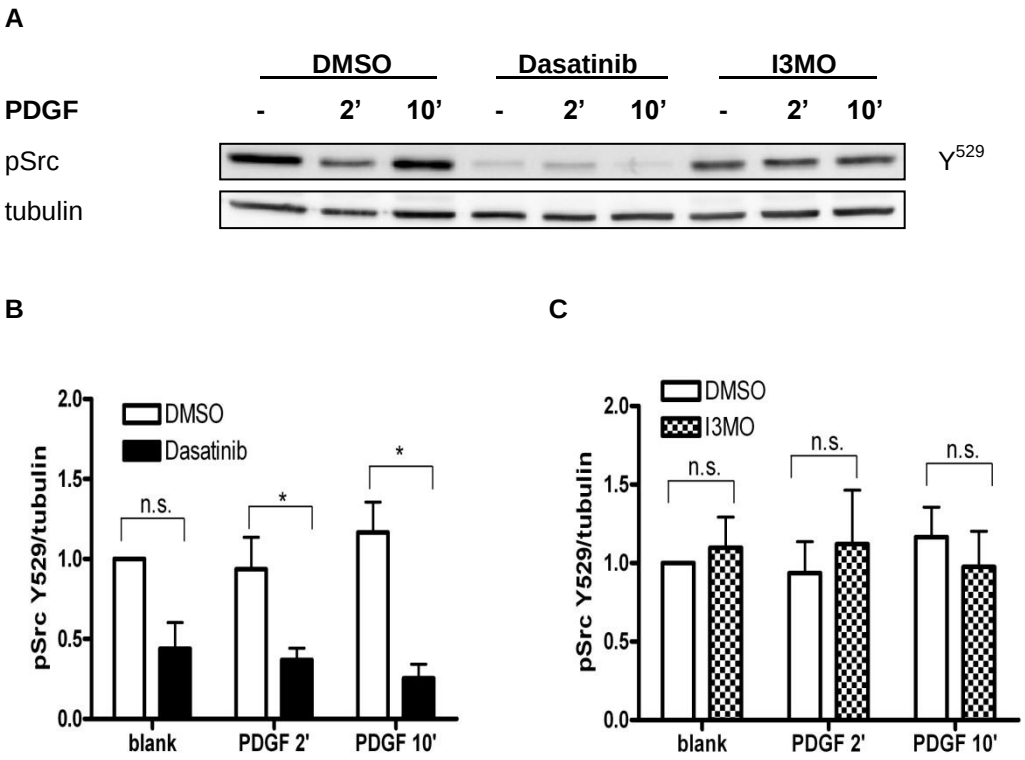

Figure 11: I3MO has no impact on phosphorylation of c-Src Y^{529} whereas dasatinib causes dephosphorylation

VSMC preincubated with I3MO 3 µM, dasatinib 100 nM and DMSO 1 %, were stimulated with 20 ng/ml PDGF-BB for up to 10 minutes. After preparing the lysates, a specific antibody against phospho-Src (Y^{529}) was used for immunoblotting; tubulin served as loading control. The experiment was performed three times. A representative western blot is shown in **(A)**. Analyzed data of treatment with I3MO is shown in **(C)** and with dasatinib in **(B)**. * $p<0.05$, n.s. (not significant) $p>0.05$ (t-test).

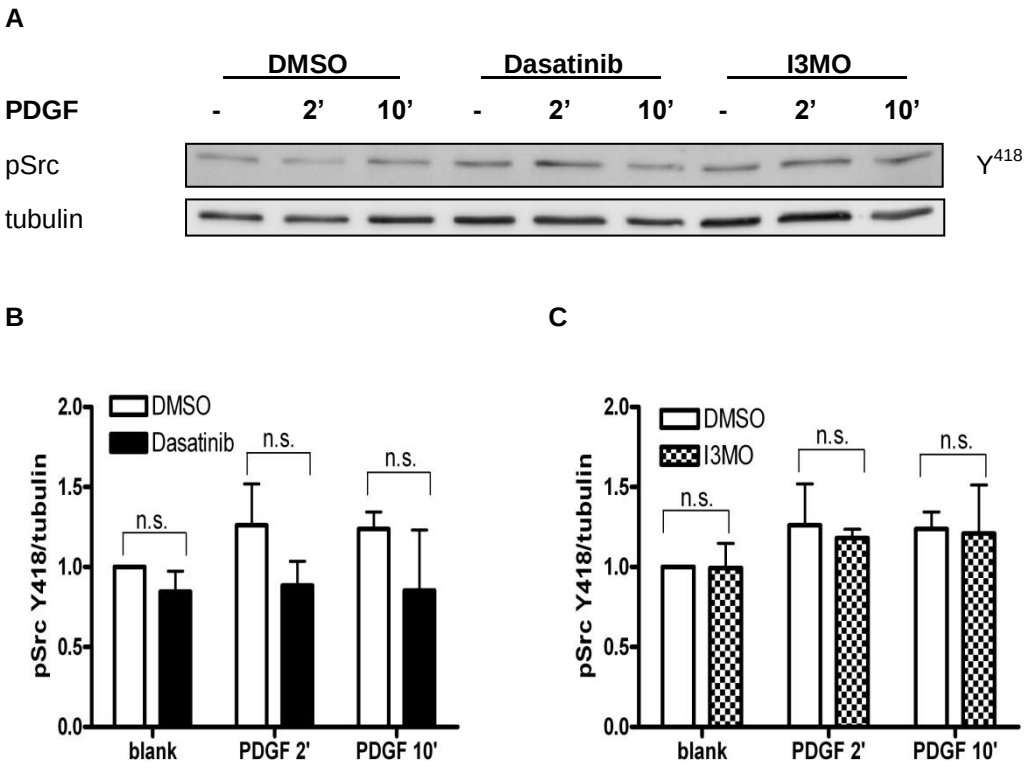

Figure 12: Dasatinib and I3MO do not affect phosphorylation of c-Src Y^{418}

Serum-starved VSMCs were preincubated for 30 minutes with I3MO 3µM, dasatinib 100 nM and DMSO 1%. After stimulation with PDGF-BB for 2 and 10 minutes, respectively, lysates were prepared as described in the Material and Method section. The experiment was repeated three times and changes in the phosphorylation status were measured densitometrically after immunoblotting with a specific antibody against phospho-Src (Y^{418}); tubulin served as loading control. A representative western blot is shown in **(A)**, analyzed data in **(B)** and **(C)**. N.s. (not significant) $p>0.05$ (t-test).

Although not having evidence for inhibition or reduction of c-Src activity via changes in the phosphorylation status of Y^{529} and Y^{418} of c-Src, we were able to observe a complete abolition of STAT3 phosphorylation, a downstream substrate of c-Src kinase, under the influence of I3MO and dasatinib in three independently performed experiments as illustrated in Fig. 13. However, statistical evaluation of the experiments surprisingly showed that the effect was not significant for dasatinib and I3MO at 2 and 10 minutes of PDGF-BB stimulation. As already mentioned when discussing the results for the PDGF-R, the reason may again be caused by interexperimental variance and subsumption of these results for statistical analysis. A representative western blot is shown in Fig.13.

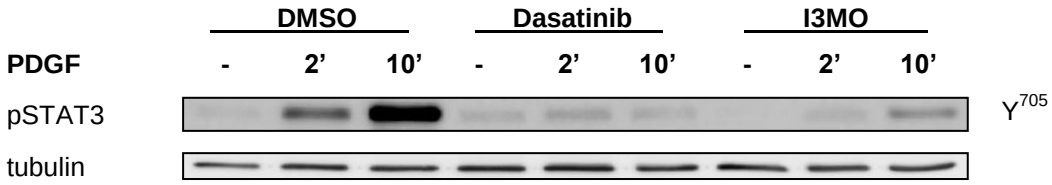

Figure 13: Dasatinib and I3MO inhibt STAT3 phosphorylation

VSMC, preincubated for 30 minutes with I3MO 3 µM, dasatinib 100 nM and DMSO 1 %, were stimulated for 2 and 10 minutes with 20 ng/ml PDGF-BB. After repeating the experiment thrice, lysates were prepared as declared in the Material and Method section. Immunoblotting was performed with a specific antibody against phospho-STAT3 (Y^{705}). A representative western blot is shown.

Fig.14 finally shows an increase of total Src protein levels after treatment with dasatinib which was monitored in all our western blots and may be explained by recruitment of Src out of cell compartiments or debonding from cell membranes. Whereas protein levels of total Src remained unaffected under the influence of I3MO. Again statistical analysis of experimental data seemed to shift western blot results from an observable increase in total Src protein levels to a non significant effect. Alteration of the experimental results, when using them for statistical analysis seems to be founded in variance of individual experimental data. To fortify our western blot results and avoid possible misapprehension when interpreting them we only illustrated the representative western blot in Fig.14 and left graphs from evaluation aside.

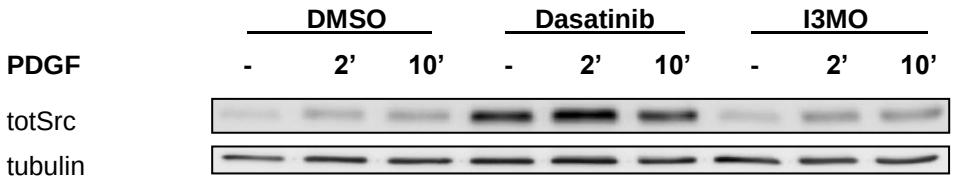

Figure 14: Dasatinib causes increase of totSrc protein level

VSMC kept serum-starved for 24 hours were stimulated with 20 ng/ml PDGF-BB after preincubating them for 30 minutes with I3MO 3 µM, dasatinib 100 nM and DMSO 1 %. Lysates were prepared according to the Materials and Methods section, afterwards a specific totSrc antibody was used for immunoblotting, with tubulin as loading control whereas a representative western blot is shown only.

4. Effect of I3MO on c-Src kinase activity

After observing an inhibition of STAT3 phosphorylation under the influence of I3MO, we carried out a second method to affirm the prior results received via western blotting in order to exclude the eventuality of c-Src not being a target of I3MO, by performing an *in vitro* tyrosine kinase assay and measuring kinase activity in the presence and absence of I3MO.

The assay, based on a phosphorylation reaction of tyrosine residues of a substrate peptide followed by detection via chemiluminescence after addition of a HRP-labelled anti-phospho-Tyr antibody, was performed with immunoprecipitated Src from VSMCs, MEF and MCF-7 lysates *(experiments no.1 – 4, see table 21 - 24)* and recombinant enzyme in solution *(experiments no.5 – 11, see table 25 and figures 15 - 18).*

In our first experiment we tried to confirm the activation of c-Src-kinase by PDGF stimulation. Because the instruction manual offered different opportunities with respect to incubation time of tyrosine kinase and its substrate, we prepared two sets of protein samples, each containing a sample of unstimulated VSMCs only treated with 1 % DMSO and another sample stimulated with 20 ng/ml PDGF-BB for ten minutes, with an overall protein concentration of 500 µg per sample. Incubation of the immunopreciptitated c-Src kinase together with its substrate peptide is required to allow direct interactions between the two proteins in terms of tyrosine residue phosphorylation of the substrate peptide. In these first experiments c-Src and its substrate were incubated for 10 and 15 minutes at 37°C, respectively.
We assumed to measure an increase of phosphorylated substrate peptide in PDGF-stimulated samples in contrast to the samples only treated with vehicle *(experiment no.1, table 21).* Although PDGF stimulation caused an increase in measured luminescence, all values were located below the values of the Reference Series implying that no substrate peptide has been phosphorylated in the samples.

These results suggest the following assumptions:

(1) we were not able to immunoprecipitate sufficient amounts of c-Src from the lysates to achieve an adequate phosphorylation of substrate peptide
(2) immunoprecipitated c-Src from cell lysates was of too low kinase activity
(3) PDGF stimulation was not sufficient to activate c-Src kinase
(4) the assay was to insensitive for an overall protein concentration of 500 µg per sample
(5) VSMCs may not be an ideal source for recruiting sufficient amounts of c-Src kinase

Due to the fact that the detected luminescence was higher after an incubation time of 10 minutes we decided to use this reaction time in all further experiments.

Sample	**Luminescence (in RLU)**
DMSO (10 minutes incubation)	9137
PDGF 10' (10 minutes incubation)	12524
DMSO (15 minutes incubation)	2130
PDGF 10' (15 minutes incubation)	4228
Ref. 0 (0 ng phosphorylated protein/µl)	14820
Ref. 1 (1 ng/µl)	32675
Ref. 2.5 (2.5 ng/µl)	40719
Ref. 5 (5 ng/µl)	41858
Ref. 10 (10 ng/µl)	47886

Table 21: Results of kinase activity experiment no.1
The instruction manual offered different opportunities to work up the samples concerning the incubation time periods of the tyrosine kinase with its substrate peptide (10 and 15 minutes).
Incubation is apprehended as the reaction between the kinase and its substrate peptide for a previously determined period (10 and 15 minutes, respectively) at 37 °C in a reaction mixture called "Master Mix",consisting of ATP, Mn and Mg.

Despite the unsatisfying results of the first experiment we decided to test the effects of different Src-kinase inhibitors in PDGF-stimulated VSMCs. Therefore five different samples were prepared:

1. VSMCs treated with 1 % DMSO as vehicle
2. VSMCs stimulated with 20 ng/ml PDGF-BB
3. VSMCs stimulated with 20 ng/ml PDGF-BB + dasatinib 100 nM
4. VSMCs stimulated with 20 ng/ml PDGF-BB + I3MO 3 µM
5. blank sample only containing lysis buffer, serving as negative control *(experiment no.2, table 22)*.

Furthermore, we increased the overall protein concentration of our samples to 1000 µg. In contrast to our first experiment we incubated all samples for ten minutes at 37°C. Because in the user manual it was declared unessential to perform the complete Reference Series for every experiment we only prepared the highest and the lowest value of the Reference Series during this experiment. Still, the results were all located below the Reference Series and additionally no increase compared to the blank value was observed, making further troubleshooting necessary.

Sample	Luminescence (in RLU)
DMSO	429
PDGF 10’	418
Dasatinib 100 nM	277
I3MO 3 µM	484
Lysis buffer	313
Ref. 0 (0 ng phosphorylated protein/µl)	1179
Ref. 10 (10 ng phosphorylated protein/µl)	88667

Table 22: Results of kinase activity experiment no.2

As first step of our troubleshooting procedure we decided to test further stimuli on VSMCs in order to investigate whether PDGF-BB was able to allow a sufficient activation of c-Src kinase. PDGF stimulation was therefore performed for different time periods (5 and 10 minutes) and, additionally, calf serum 10 % was used as stimulus. DMSO 1 % and blank lysis buffer were used as controls.
Prepared samples for tyrosine kinase assay *(experiment no.3)*:

1. VSMCs with 1 % DMSO (vehicle)
2. VSMCs stimulated with 20 ng/ml PDGF-BB for 5 minutes

3. VSMCs stimulated with 20 ng/ml PDGF-BB for 10 minutes
4. VSMCs stimulated with 10 % calf serum for 10 minutes
5. blank lysis buffer.

Although values were located more inside the Reference Series, the samples stimulated with PDGF-BB for 5 and 10 minutes still did not seem to experience a sufficient stimulation of c-Src kinase and consequently to achieve higher concentrations of phosphorylated substrate peptide resulting in a significant increase of luminescence compared to the blank value. Calf serum failed as stimulus.

Sample	Luminescence (in RLU)
DMSO	3316
PDGF 5’	3742
PDGF 10’	4114
Calf Serum 10%	2350
Lysis buffer	2747
Ref. 0	3675
Ref. 10	68163

Table 23: Results of kinase activity experiment no.3

The next kinase assay experiment *(experiment no.4, table 24)* was not only performed with VSMCs, but also with MEF (mouse embryonic fibroblasts) and MCF-7 breast cancer cells, two cell lines assumed to contain higher amounts of c-Src compared to VSMCs. Moreover, we used a specific lysis buffer (CHAPS buffer) in addition to our commonly used buffer because of its ability to make even membrane proteins accessible. The experiment was performed with cells directly harvested from culture conditions lacking serum starvation and PDGF-BB treatment; blank lysis buffer was used as control.

Similar to the previous experiments, all samples seem to miss an adequate activation of c-Src kinase, resulting in luminescene values located below the Reference Series. Even the used CHAPS buffer was not able to recruit sufficient amounts of c-Src from VSMCs and the other cell types, actually it seemed to be less

effective in VSMCs than our commonly used lysis buffer. In contrast, samples received with the CHAPS buffer seemed to cause slightly higher c-Src kinase activity in MCF-7 and MEF cells compared to lysates received with our common buffer.

Sample	Lysis buffer	Luminescence (in RLU)
MCF-7	CHAPS buffer	2704
MEF		3324
VSMC		510
MCF-7	Common lysis buffer	940
MEF		2714
VSMC		1686
Lysis buffer		745
Ref. 0		5204
Ref. 10		38330

Table 24: Results of kinase assay experiment no.4

Due to the recieved results, not able to provide sufficient kinase activity even with increased protein concentrations, different stimuli and other cell lines, we decided to perform the next experiments with recombinant, active c-Src. Our first experiment was performed to empirically determine the concentration of recombinant enzyme allowing us to perform reproducible experiments *(experiment no.5, table 25)*; kinase activity was measured in increasing concentrations from 10 – 100 ng.

Sample	Luminescence (in RLU)
c-Src 10 ng	1076
c-Src 25 ng	964
c-Src 50 ng	670
c-Src 100 ng	861
Ref. 0	250
Ref. 10	20890

Table 25: Results of kinase assay experiment no.5

Although the first results using the recombinant enzyme were promising, we performed an additional experiment with an enzyme concentration of 500 ng to gain wider margin to avoid descending below the Reference Series when using an inhibitor.

The following samples were prepared *(experiment no.6):*

1. c-Src 100ng
2. c-Src 500ng
3. c-Src 500ng + DMSO 1%
4. c-Src 500ng + I3MO 3µM
5. blank Master Mix as control

We were able to observe a decrease of c-Src kinase activity with I3MO 3 µM, however, the luminescence level of our sample was below the level of blank Master Mix (a reaction mixture containing ATP, Mn, Mg and the recombinant enzyme to create an environment enabling the phosphorylation of the substrate peptide), so we were not able to clearly determine the extent of kinase activity reduction.

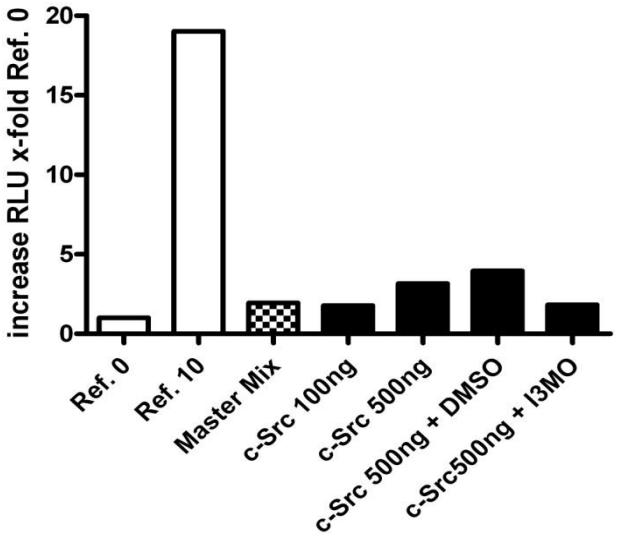

Figure 15: Results of tyrosine kinase assay no.6

For the next experiment we prepared two identical sets of samples with c-Src 100 ng and 500 ng and a complete Reference Series for each set of samples *(experiment no.7, Fig. 16).* After evaluation of the achieved results we finally decided to perform all future experiments with a concentration of 500 ng of active c-Src because of the higher levels of phosphorylated substrate.

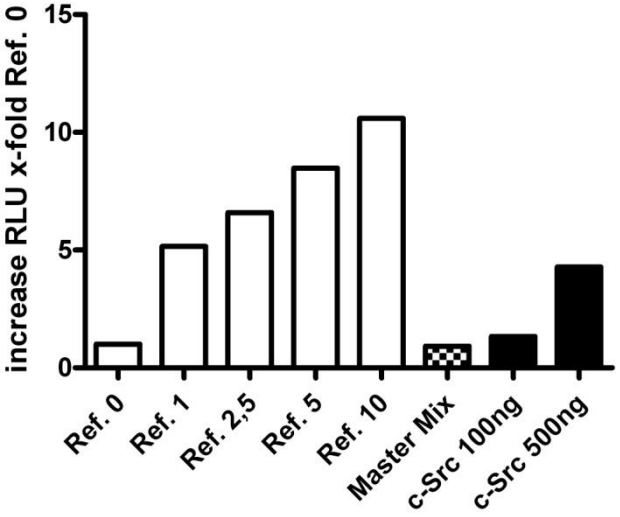

Figure 16: Results of kinase assay experiment no.7

Shown are the average results received from two parallel performed experiments.

After finding of a sensitive setting for our experiments we were finally able to investigate potential inhibitory effects of I3MO 3 µM on Src-kinase activity. Therefore the following three experiments were performed in the same setting with a complete Reference Series *(experiments no.8-10, see Fig. 17)*:

1. c-Src 500ng
2. c-Src 500ng + DMSO 1%
3. c-Src 500ng + I3MO 3µM
4. Ref. 0 (0 ng/µl phosphorylated Reference peptide)
5. Ref. 1 (1 ng/µl phosphorylated Reference peptide)
6. Ref. 2.5 (2.5 ng/µl phosphorylated Reference peptide)
7. Ref. 5 (5 ng/µl phosphorylated Reference peptide)
8. Ref. 10 (10 ng/µl phosphorylated Reference peptide)

In all three performed experiments we were able to observe an inhibition of kinase activity, varying from 20 – 80 % of reduction. Additionally we determined the R-values from the Reference Series performed from experiment 7 – 11, which spread from 0.6434 to 0.9558.

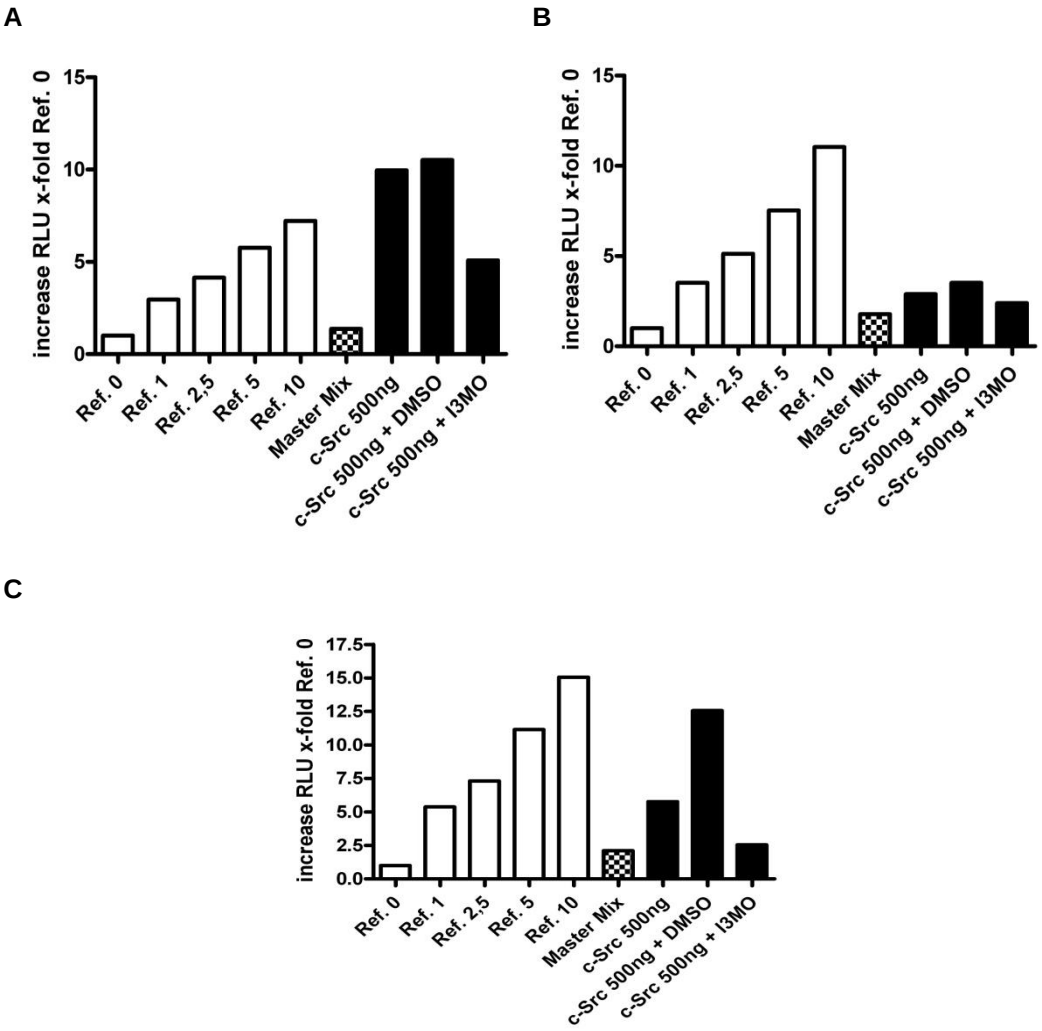

Figure 17: Results of kinase assay experiments no.8-10

Shown is the x-fold increase of relative light units (RLU) compared to Ref. 0 of experiment no.8 **(A)**, experiment no.9 **(B)** and experiment no.10 **(C)**; blank Master Mix was used as control and a representative Reference Series from experiment no.9 is shown **(D)**.

In our final experiment *(no.11, see Fig. 18),* we tried to exclude all possible interactions of DMSO and I3MO with the Master Mix and possible inhibitory effects of I3MO concerning the biotin-streptavidin interactions necessary to bind the substrate peptide to the 96-well microplate for phosphorylation. In addition to the samples used to perform in experiments no. 8 – 10 we prepared a sample with Master Mix and DMSO or I3MO, respectively; additionally, a sample with reference substrate [10 ng/µl (Ref. 10)] with I3MO was prepared. Again kinase activity was inhibited by I3MO 3µM, whereas DMSO showed no reduction of c-Src kinase activity. Additionally, DMSO and I3MO did not show any substantial interactions with the Master Mix. I3MO also does not seem to inhibit biotin-streptavidin interactions, instead it rather seems to increase the amount of phosphorylated protein.

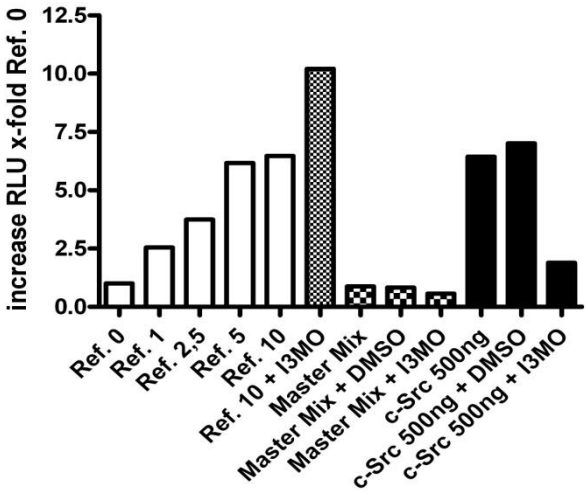

Figure 18: Results of kinase assay experiment no.11

In our final tyrosine kinase assay we initially tried to repeat the inhibition of c-Src kinase activity by I3MO, which we already observed in previous experiments; DMSO had no impact on measured kinase activity. Additionally, we tried to confirm the absence of potential interactions between the Master Mix and I3MO as well as DMSO during incubation by preparing additional samples only consisting of Master Mix and I3MO or DMSO, respectively.

Finally we identified the average of kinase activity inhibition from all comparable performed kinase assay experiments *(experiments no.6, 8, 9, 10 and 11)*, in which

we were able to detect an average reduction of kinase activity of about 50 %. Examining each experiment individually, the percental inhibition ranged from 20 – 70 %.

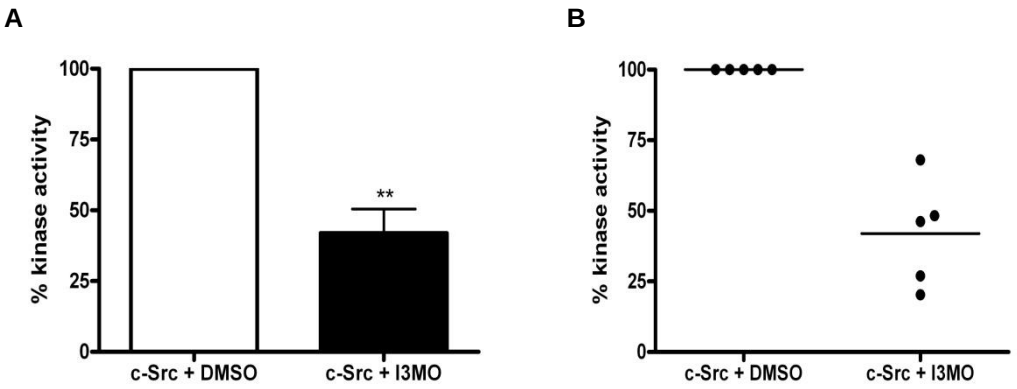

Figure 19: Average inhibition of kinase activity by I3MO

The average kinase activity after treatment with I3MO 3 µM remains at about 50 %. When looking at each experiment separately, the inhibition ranged from 20 – 70 %.

Shown are the average inhibition of Src-kinase activity **(A)** and inhibition examined from each experiment separately **(B)**. ** $p<0.005$ (t-test).

5. Antioxidants in PDGF signalling

According to previous studies, antioxidants and other antioxidative active compounds seem to exert a beneficial effect in preventing the development of cardiovascular diseases. [27,42] While for some, like lycopene, the mechanism in mediating the beneficial effect on prevention of CVDs is still largely unknown [27], a large number of additional as well as independent effects from their antioxidative activity has been identified for polyphenolic compounds (e.g. green tea catechins).[42] Especially the antioxidants ability to inhibit PDGF-induced signalling cascades, which has already been shown for EGCG [3,45], a green tea catechin and polyphenol respectively, and lycopene [27], a natural compound from tomato, was of particular interest. Independent from these findings another antioxidant, resveratrol, has proven to be able to inhibit Src and STAT3 signalling in v-Src transfected NIH3T3 mouse fibroblasts.[24]

Considering the results of these studies, we examined the effects of three further antioxidants, ascorbic acid (dissolved in distilled water), dehydroascorbic acid (dissolved in DMSO) and trolox (dissolved in ethanol 100%) on PDGF-induced signalling cascades regarding their potential inhibitory effects by measuring the phosphorylation status of the PDGF-R and other signalling molecules involved in PDGF signalling like STAT3, Erk1/2, p38 MAPK and Akt.

For the performance of these experiments 24 h serum-starved VSMCs were preincubated 1 hour with the antioxidants in a concentration of 100 nM and afterwards stimulated with 20 ng/ml PDGF-BB for the declared time periods. To exclude possible effects on VSMCs resulting from the solvents, VSMCs preincubated for 1 h with blank solvent were prepared for comparison. Unstimulated samples, only treated with the different solvents, served as controls.

The results of the performed experiments can be subsumed in the following way. None of the three antioxidants seems to inhibit or somehow affect the activation of p38 MAPK, Akt or Erk1/2 kinases. Their effects on activation of STAT3 and

phosphorylation of the PDGF-R remain indistinct, because of serious discrepancies between the particular experiments.

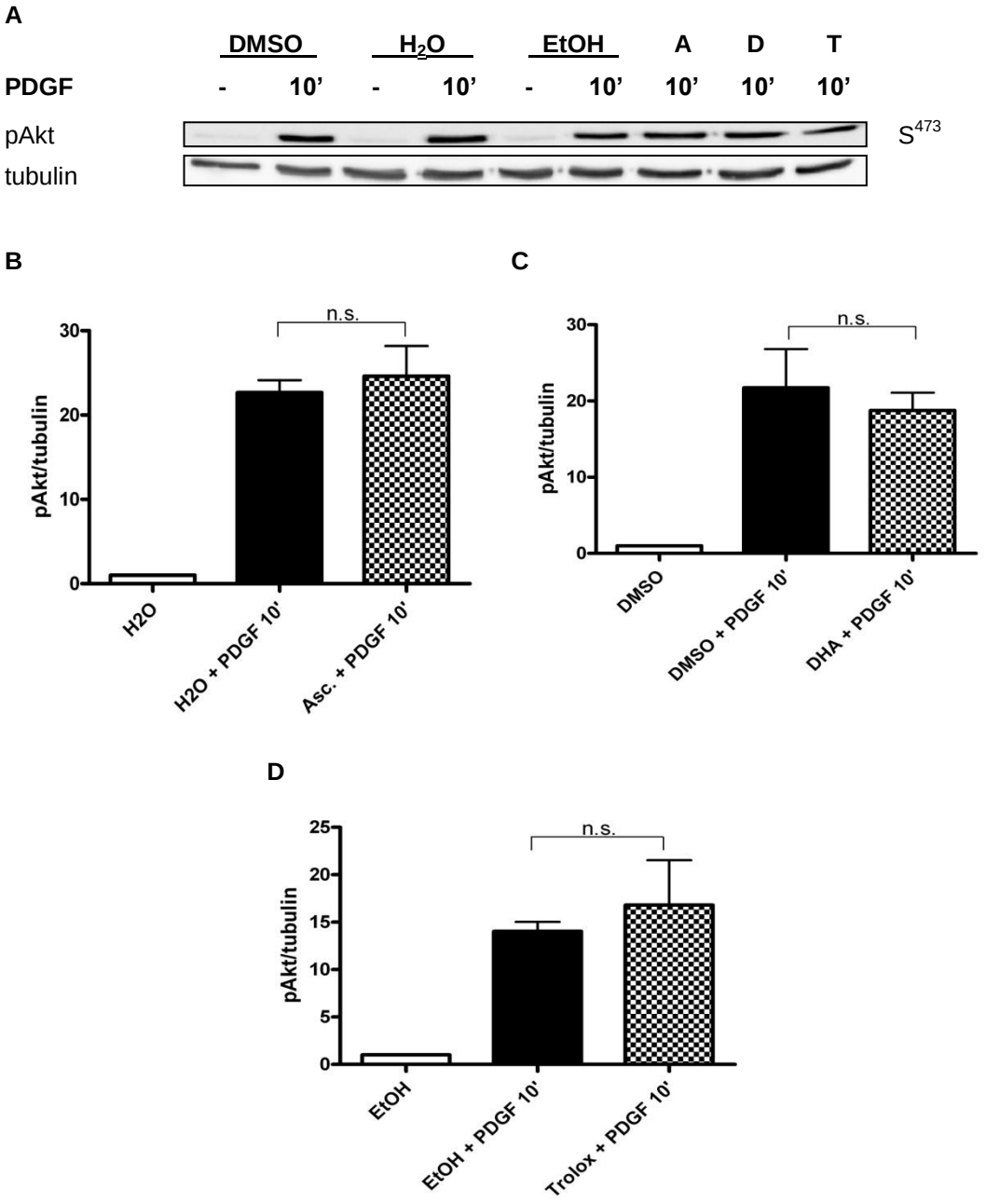

Figure 20: Ascorbic acid, dehydroascorbic acid and Trolox do not inhibit Akt kinase phosphorylation
24 hour serum-starved VSMC were preinucbated with ascorbic acid 100 nM (A), dehydroascorbic acid 100 nM (D), trolox 100 nM (T) or vehicles for one hour. Lysates were prepared as declared in the Materials and Method section. For Immunoblotting a specific antibody against phospho-Akt (S^{473}) was used; tubulin served as loading control. The experiment was performed in triplicate. Shown are one representative western blot selected from the three

experiments **(A)** and changes in phosphorylation levels after treatment with ascorbic acid **(B),** dehydroascorbic acid **(C)** and trolox **(D)**. Blank solvents were used as control to exclude potential inhibitory effects from the solvents. n.s. (not significant) p>0.05 (t-test).

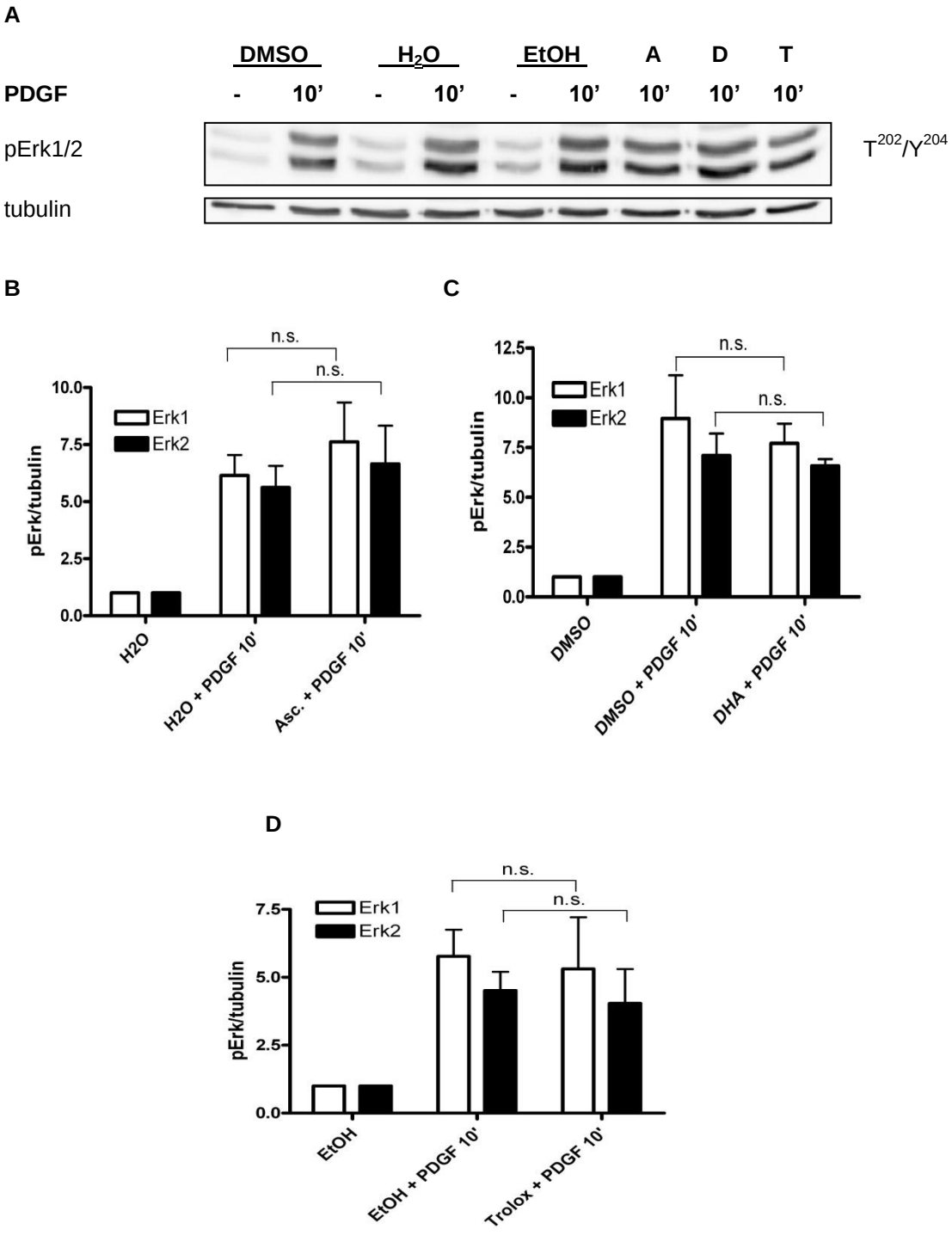

Figure 21: Ascorbic acid, dehydroascorbic acid and trolox have no impact on Erk1/2 phosphorylation

Serum-starved VSMC were stimulated with PDGF-BB for ten minutes after one hour of preincubation with the antioxidants ascorbic acid 100 nM (A), dehydroascorbic acid 100 nM (D), trolox 100 nM (T) or vehicles. After preparing the lysates as described in the Material and Method section, a specific antibody against phospho-Erk1/2 (T^{202}/Y^{204}) was used for immunoblotting. The experiment was repeated three times and a representative western blot is shown in **(A)**. The graphs received after densitometric analysis of the experimental results show no impact of ascorbic acid **(B)**, dehydroascorbic acid **(C)** and trolox **(D)** on phosphorylation of Erk1/2 kinases. n.s. (not significant) p0.05 (t-test).

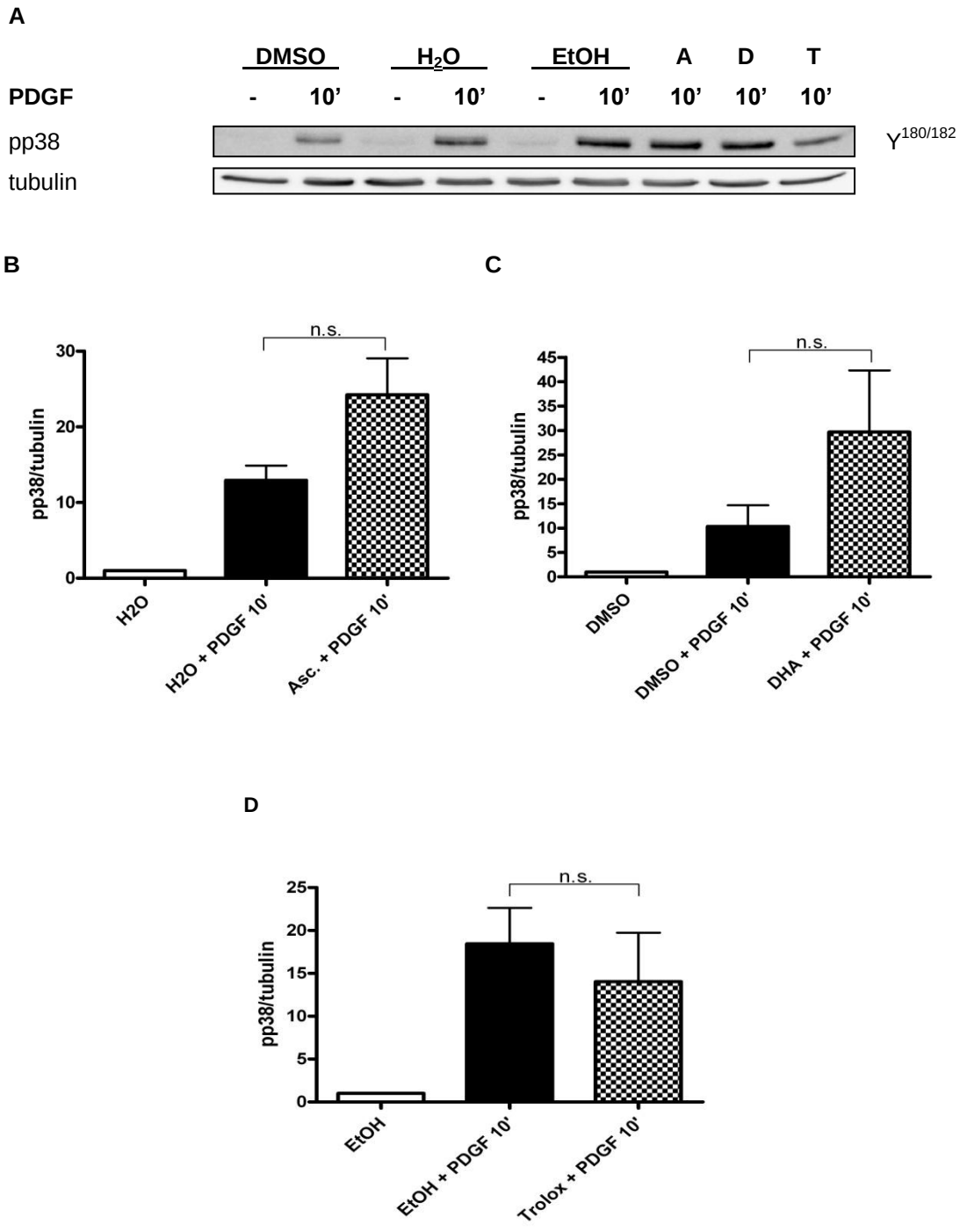

Figure 22: Ascorbic acid, dehydroascorbic acid and trolox have no effect an p38 phosphorylation/activation

After preincubating serum-starved VSMC for one hour with ascorbic acid 100 nM (A), dehydroascorbic acid 100 nM (D) and trolox 100 nM (T) they were stimulated with PDGF-BB for ten minutes. After preparing the lysates as described in the Material and Methods section, a specific antibody against phospho-p38 ($Y^{180/182}$) was used for immunoblotting. The representative western blot **(A)** and graphs show no inhibitory effects on

p38 phosphorylation caused by ascorbic acid **(B)**, dehydroascorbic acid **(C)** and trolox **(D)**, compared to their vehicles after stimulation with PDGF-BB. Blank vehicles were used as control. n.s. (not significant) $p>0.05$ (t-test).

E DISCUSSION

E Discussion

1. Introduction

Abnormal proliferation of VSMCs is one of the key events in the development of atherosclerosis and even restenosis after initial successful coronary angioplasty.[27] Of vital importance within this complex process is PDGF, serving as a major mitogen for VSMCs, responsible for their migration and increased proliferation.[17,19] Thus, inhibition of aberrant PDGF-induced VSMC proliferation seems to be a promising alternative for today's commonly used strategies to treat atherosclerosis, including PTCA and stent implantation. Indirubin, the active principle of a TCM anti-leukaemic recipe[20], and its derivatives, especially I3MO[23], represent potent antiproliferative compounds due to their inhibition of inflammatory[37] and oncogenic[30] pathways. In VSMCs, I3MO was shown to exhibit an inhibitory effects on STAT3 activation, PDGF-R phosphorylation, and ROS production.[36] Considering STAT3 as a downstream substrate of the non-receptor tyrosine kinase c-Src[6], we tried to clarify whether the inhibition of c-Src kinase activity is the basic cause for subsequent abolition of STAT3 phosphorylation.

2. PDGF-R autophosphorylation

The initial step to activate downstream signalling pathways of PDGF is autophosphorylation of the PDGF-R. Phosphorylated tyrosine residues create binding sites for SH2-domain containing adaptor proteins and other singaling molecules, leading to further phosphorylation/activation of their downstream substrates.[18,19] Inhibition of phosphorylation of specific tyrosine residues therefore prevents creation of these binding pockets and subsequently activition of downstream substrates. In our experiments we were able to show a reduced overall phosphorylation of the PDGF-R under the influence of dasatinib and I3MO at 2 and 10 minutes of PDGF stimulation. In earlier studies the same effect has already been described for I3MO regarding PDGF-R phosphorylation in total and particularly on $Y^{579/581}$.[36] Considering that phosphorylation of $Y^{579/581}$ is necessary for c-Src activation and further activation of its downstream substrates[9,18], we investigated a possible inhibitory effect of I3MO on Src kinase activity.

3. MAPK- and PI3K-pathway

Other important pathways involved in PDGF signalling are the MAPK- and the PI3K-pathway. Binding of the Grb2/Sos1 complex to PDGF-R leads to activation of Ras, which in turn causes activation of MAPKKK Raf1. Raf1 itself induces phosphorylation of MEK1/2, which activate Erk1/2 by phosphorylating threonine and tyrosine residues. Erk1/2 cause VSMC proliferation by transcription of intermediate early genes like c-myc and c-fos induced via phosphorylation and translocation of Elk1 and p90RSK.[15, 39]

To exclude these two pathways from containing potential new targets of I3MO we performed time courses in the presence and absence of I3MO, measuring the phosphorylation status of Erk1/2 and Akt kinase at different time periods after PDGF stimulation. I3MO treatment did not lead to any changes in the phosphorylation status of Akt kinase, confirming the results previously shown.[36] Phosphorylation of Erk1/2 kinases was diminished at 2 minutes of PDGF stimulation in the presence of I3MO, but returned to physiological levels after 5 minutes of PDGF stimulation. We therefore reconfirmed that MAPK- and PI3K-pathway are not affected by I3MO, indicating that the cell system worked as previously shown.

4. c-Src kinase

Binding of c-Src via its SH2-domain to phosphorylated PDGF-R is involved in activation of the kinase. Changes in the phosphorylation status of the two tyrosine residues Y^{418} and Y^{529} regulate the kinase activity of c-Src.[19, 35] Phosphorylation of Y^{418} causes increased kinase activity by dislocating Y^{418} from the kinase substrate binding pocket, allowing substrates better access.[5] Increased phosphorylation of Y^{529} instead causes enhanced interactions of Y^{529} with the kinases SH2-domain, forcing its transformation into the inactive conformation.[5,34] However, in our time courses, I3MO seems not to affect the phosphorylation of both tyrosine residues, except of a diminished phosphorylation of Y^{529} after 2 minutes of PDGF stmulation, similarly to the results obtained with Erk1/2 kinases, and was therefore classified as inconsiderable. A different view is obtained with dasatinib. Although not affecting the phosphorylation of Y^{418}, a clear inhibition of Y^{529} phosphorylation could be observed. When examining the expressed protein levels of total Src, we observed increased

protein levels under treatment with dasatinib, not seen with I3MO. Summarised, the results did not indicate an effect of I3MO on phosphorylation status of Y^{418} and Y^{529}.

5. STAT3

STAT3 is known to be one of the downstream substrates of Src-kinase and has already been identified as a target of I3MO in earlier studies.[6,30] With our experiments we were able to confirm the inhibition of STAT3 phosphorylation with I3MO as well as with dasatinib. Due to inhibition of STAT3 activation and its nature as a downstream substrate of Src-kinase, we hypothesized an inhibition of Src-kinase activity as reason for the inhibition of STAT3 phosphorylation.

6. c-Src kinase activity

To confirm our assumption of I3MO inhibiting STAT3 activation via Src kinase inhibition we performed a tyrosine kinase assay to measure kinase activity after PDGF stimulation and I3MO treatment. Due to the fact that we were not able to illustrate an explicit inhibitory effect of I3MO on activated c-Src neither immunoprecipitated from VSMC lysates nor MEF or MCF-7 lysates, further *in vitro* tyrosine kinase assays were conducted with recombinant activated human c-Src. Pooled data from five performed experiments showed an average inhibition of kinase activity under I3MO treatment of about 50 %, compared to PDGF stimulation. The kinase activity was ranging from 20 – 70 % when looking at each experiment separately. Although these results seem very promising at first sight it has to be kept in mind, that no comparable effect was observed or reproducible in any of the previously performed western blot experiments. Not even *in vitro* tyrosine kinase assays performed with c-Src from cell lysates were able to show an approximate outcome. Therefore existing inconsistency within the available results does not deliver any verification of coherence between the observed inhibition of tyrosine kinase activity in cell free conditions and potential influences of I3MO in the cellular model. Furthermore, when considering the consequences of changes in experimental setting like switching from immunoprecipitated c-Src from cell lysates to recombinant c-Src, potential effects of I3MO on c-Src kinase activity and its downstream cellular signalling may not be predicted for in vivo conditions at the moment.

7. Antioxidants

Antioxidants are widely known to deploy benefic effectsial on prevention of CVDs[27] and other malignant proliferative diseases[3,42]. Especially their effects on PDGF-induced signalling and the involved signalling molecules are of vital importance when considering the relevance of their antiproliferative effects, which some of them, especially EGCG[3,45], exert on VSMCs.[24,27]

Initiated by these findings, we focused on the examination of three widely known antioxidants, ascorbic acid, dehydroascorbic acid and trolox, regarding a potential beneficial impact in preventing development of CVDs by inhibition of VSMC proliferation due to inference with PDGF-induced signalling cascades.

Anyhow, summarized data from our western blots did not show any changes in the phosphorylation status, correlating with activity, of essential signalling molecules like Akt kinase, Erk 1/2 kinases or $p38^{MAPK}$ regardless of the presence or absence of the antioxidants. Considering the remaining evaluable results it currently seems that the investigated antioxidants do not deploy a beneficial effect on the prevention of CVDs by interfering with PDGF-induced signalling. Furthermore, it has to be mentioned that prevention of CVDs like atherosclerosis by these antioxidants may not result from inhibition of disease development or progression via repression of VSMC proliferation, but maybe from preventing ROS-induced vascular wall injury.

8. Conclusion

Prior studies identified I3MO to be capable to inhibit PDGF-R overall phosphorylation, PDGFR $Y^{579/581}$ phosphorylation, STAT3 phosphorylation and c-Src kinase signalling.[30,36] Nevertheless, its effect on c-Src kinase activity in VSMCs has not been determined so far. As previously shown, we were also able to observe a significant inhibition of PDGF-R autophosphorylation and STAT3 activation *in vitro*, assuming an upstream molecule of STAT3 as possible target for I3MO. Considering the before mentioned ability of I3MO to inhibit PDGFR $Y^{579/581}$ autophosphorylation, which is crucial for creation of binding sites for SH2 domain-containing downstream signalling molecules activated by the PDGF-R, particularly for c-Src kinase as one of them, a diminished phosphorylation of PDGFR $Y^{579/581}$ could deliver a possible explanation for reduced c-Src kinase activity and consequent interruption of STAT3 signalling under I3MO treatment. In the *in vitro* tyrosine kinase assay, performed

with recombinant, active c-Src in cell free environment we observed an average reduction of kinase activity of around 50% in presence of I3MO indicating that Src represents a potential target of I3MO. However, these results were only received under *in vitro* conditions, outside the physiologic environment and are therefore not necessarily assignable to cellular conditions. Further experiments are required to elucidate the effect of I3MO on c-Src kinase in the cellular system as well as under *in vivo* conditions.

F REFERENCES

F References

1. Abram, C.L. & Courtneidge, S.A. Src family tyrosine kinases and growth factor signaling. *Exp Cell Res* **254,** 1 – 13 (2000)

2. Adachi, J. et al. Comparism of gene expression patterns between 2,3,7,8-tetrachlorodibenzo-p-dioxin and a natural arylhydrocarbon receptor ligand, indirubin. *Toxicol Sci* **80**, 161 – 9 (2004)

3. Ahn, H.Y. et al. Epigallocatechin-3-gallate selectively inhibits the PDGF-BB-induced intracellular signalling transduction pathway in vascular smooth muscle cells and inhibits transformation of sis-transfected NIH 3T3 fibroblasts and human glioblastoma cells (A172). *Mol Biol Cell* **10**,1093 – 1104 (1999)

4. Andrae, J., Gallini, R., & Betsholtz C. Role of platelet-derived growth factors in physiology and medicine. *Genes & Dev* **22**, 1276 – 1312 (2008)

5. Bjorge, J.D., Jakymiw, A. & Fujita, D. J. Selected glimpses into the activation and function of Src kinase. *Oncogene* **19**, 5620 – 35 (2000)

6. Bowman, T. et al. STAT3-mediated Myc expression is required for Src transformation and PDGF-induced mitogenesis. *Proc Natl Acad Sci* **98**, 7319 – 24 (2001)

7. Cantley L.C. The phosphoinositide 3-kinase pathway. *Science* **296**, 1655 – 7 (2002)

8. Chang, Y.M., Kung, H.J. & Evans, C.P. Nonreceptor tyrosine kinases in prostate cancer. *Neoplasia* **9**, 90 – 100 (2007)

9. Claesson – Walsh, L. Platelet-derived growth factor receptor signals. *J Biol Chem* **269**, 32023 – 26 (1994)

10. Dancey J.E. Therapeutic targets: MTOR and related pathways. *Cancer Biol Ther* **9**, 1065 – 73 (2006)

11. Dzau, V.J., Braun-Dullaeus, R.C. & Sedding, D.G. Vascular proliferation and atherosclerosis: New perspectives and therapeutic strategies. *Nat Med* **8**, 1249 – 56 (2002)

12. Ebong, S. et al. Activation of STAT signalling pathways and induction of suppressors of cytokine signalling (SOCS) proteins in mammalian lens by growth factors. *IOVS*, **45**, 872 – 8 (2004)

13. Eisenbrand, G. et al. Molecular mechanisms of indirubin and its derivatives: novel anticancer molecules with their origin in traditional Chinese phytomedicine. *J Cancer Clin Oncol* **130**, 627 – 35 (2004)

14. Engelman, J.A., Luo, J. & Lewis, C.C. The evolution of phosphatidylinositol 3-kinases as regulators of growth and metabolism. *Nat Rev Genet* **7**, 606 – 19 (2006)

15. Fang, J.Y. & Richardson, B.C. The MAPK signalling pathway and colorectal cancer. *Lancet Oncol* **6,** 322 – 27 (2005)

16. Farago, M. et al. Kinase-inactive glycogen synthase kinase 3ß promotes Wnt signalling and mammary tumorigenesis. *Cancer Res* **65**, 5762 – 5801 (2005)

17. Fredriksson, L., Li, H., & Eriksson, U. The PDGF family: four gene products form five dimeric isoforms. *Cytokine Growth Factor Rev* **15**, 197 – 204 (2004)

18. Heldin, C.H., Östman, A. & Rönnstrand L. Signal transduction via platelet-derived growth factor receptors. *Biochim Biophys Acta* **1378**, F79 – F113 (1998)

19. Heldin, C.H. & Westermark, B. Mechanism of action and in vivo role of platelet-derived growth factor. *Physiol Rev* **79**, 1283 – 1316 (1999)

20. Hoessel, R. et al. Indirubin, the active constituent of a Chinese antileukaemia medicine, inhibits cyclin-dependent kinases. *Nat Cell Bio* **1**, 60 – 7 (1999)

21. Ishizawar, R. & Parsons, S.J. c-Src and cooperating partners in human cancer. *Cancer Cell* **6**, 209 – 14 (2004)

22. Jiang, B.H. & Liu L.Z. PI3K/PTEN signalling in tumorigenesis and angiogenesis. *Biochim Biophys Acta* **1784**, 150 – 8 (2008)

23. Kim, S.A. et al. Antitumor activity of novel indirubin derivatives in rat tumor model. *Clin Cancer Res* **13**, 253 – 9 (2007)

24. Kotha, A. et al. Resveratrol inhibits Src and STAT3 signalling and induces apoptosis of malignant cells containing activated STAT3 protein. *Mol Cancer Ther*, **5**, 621 – 29 (2006)

25. Kumar, V., Abbas, A.K. & Fausto, N. Pathologic basis of disease. **7th Edition**, 511 -524 (2005)

26. Li, S. Src kinase signalling in leukaemia. *Int J Biochem Cell Biol* **39**, 1483 – 88 (2007)

27. Lo, H.M. et al. Lycopene binds PDGF-BB and inhibits PDGF-BB-induced intracellular signalling transduction pathway in rat smooth muscle cells. *Biochem Pharmacol* **74**, 54 – 63 (2007)

28. Lusis, A.J. Atherosclerosis. *Nature* **407**, 233 – 41 (2000)

29. Nam, S. et al. Action of the Src family kinase inhibitor, dasatinib (BMS-354825) on human prostate cancer cells. *Cancer Res* **65**, 9185 – 9 (2005)

30. Nam, S. et al. Indirubin derivatives inhibit STAT3 signaling and induce apoptosis in human cancer cells. *Proc Natl Acad Sci* **102**, 5998 – 6003 (2005)

31. Nam, S. et al. Dasatinib (BMS-354825) inhibits STAT5 signaling associated with apoptosis in chronic myelogenous leukemia cells. *Mol Cancer Ther* **6**, 1400 – 5 (2007)

32. Olivieri, A. & Manzione, L. Dasatinib: a new step in molecular target therapy. *Ann Oncol* **18**, vi42 – 6 (2007)

33. Raines, E.W. PDGF and cardiovascular disease. *Cytokine Growth Factor Rev* **15**, 237 – 54 (2004)

34. Roskoski, R. Jr. Src protein-tyrosine kinase structure and regulation. *Biochem Biophys Res Commun* **324**, 1155 – 64 (2004)

35. Roskoski, R. Jr. Src kinase regulation by phosphorylation and dephosphorylation. *Biochem Biophys Res Commun* **331**, 1 – 14 (2005)

36. Schwaiberger, A.V. Studies on the molecular mechanism of indirubin-3'-monoxime regarding its antiproliferative effect in vascular smooth muscle cells. *PhD thesis* (2008)

37. Sethi, G. et al. Indirubin enhances tumor necrosis factor-induced apoptosis through modulation of nuclear factor-κB signalling pathway. *J Biol Chem* **281**, 23425 – 35 (2006)

38. Shah, N.P. Medical management of CML. *Hematology Am Soc Hematol Educ Program*, 371 – 5 (2007)

39. Shaul, Y.D. & Seger R. The MEK/ERK cascade: from signalling specificity to diverse functions. *Biochim Biophys Acta* **1773**, 1213 – 26 (2007)

40. Shor, A.C. et al. Dasatinib inhibits migration and invasion in diverse human sarcoma cell lines and induces apoptosis in bone sarcoma cells dependent on Src kinase for survival. *Cancer Res* **67**, 2800 – 8 (2007)

41. Silva, C.M. & Shupnik, M.A. Integration of steroid and growth factor pathways in breast cancer: focus on signal trasnducers and activators of transcription and their potential role in resistance. *Mol Endocrinol* **21**, 1499 – 1512 (2007)

42. Stoclet, J.C. et al. Vascular protection by dietary polyphenols. *Eur J Pharmacol* **500**, 299 – 313 (2004)

43. Summy, J.M. & Gallick, G.E. Treatment for advanced tumors: Src reclaims center stage. *Clin Cancer Res* **12**, 1398 – 1401 (2006)

44. Valgeisdóttir, S. et al. Activation of STAT5 by platelet-derived growth factor is dependent on phosphorylation sites in PDGF ß-receptor juxtamembrane and kinase insert domain. *Oncogene*, **16**, 505 – 15 (1998)

45. Weber, A.A. et al. Mechanism of the inhibitory effects of epigallocatechin-3 gallate on platelet-derived growth factor-BB-induced cell signalling and mitogenesis. *FASEB J* **18**, 128 – 30 (2004)

46. Yang, K. et al. Glycogen synthase kinase 3 has a limited role in cell cycle regulation of cyclin D1 levels. *BMC Cell Biol* **7**, 33 (2006)

47. Yang, S. & Roux, B. Src kinase conformational activation: thermodynamics, pathways and mechanisms. *PLoS Comput Biol* **4**, 1 – 14 (2008)

48. Yu, J., Ustach, C. & Kim, H.R. Platelet-derived growth factor signalling and human cancer. *J Biochem Mol Bio* **36**, 49 – 59 (2003)

49. Zheng, X. Et al. Reciprocal t(9;22) ABL/BCR fusion proteins: laukogemic potential and effects on B cell commitment. *PLoS One* **10**, 1 – 11 (2009)

G APPENDIX

G APPENDIX

1. Abbreviations

A

AhR	Aryl hydrocarbon receptor
APS	Ammonium persulphate
ATP	Adenosine triphisphate

B

B-ALL	B-cell acute lymphoblastic leukaemia
BAD	Bcl-2 antagonist of cell death
Bcl-2	B-cell lymphoma 2
Bcl-X_L	B-cell lymphoma extra large
Bcr	Breakpoint cluster region
BSA	Bovine serum albumin

C

CDK	Cyclin-dependent kinase
CHAPS	3-[(3-Cholamidopropyl)dimethylammonio]-1-propanesulfonate
CHD	Coronary heart disease
CHK	CSK homologous kinase
CML	Chronic myeloic leukaemia
CSF	Colony stimulating factor
CSK	c-Src kinase
CYP	Cytochrom P 450

D

DAG	Diacylglycerol
DHFR	Dihydrofolate reductase
DMSO	Dimethylsulphoxide
DNA	Desoxyribonucleic acid
DTT	Dithiothreitol

E

EC	Endothelial cell
ECL	Enhanced chemiluminescence
ECM	Extracellular matrix
EDTA	Ethylendiamintetraacetic acid
EGF	Epidermal growth factor

EGTA	Ethylene glycol-bis(2-aminoethylether)-tetraacetic acid
ELISA	Enzyme-linked immunosorbent assay
Erk	Extracellular signal-regulated kinase
EtOH	Ethanol

F

5‘-FIO	5‘-fluoro-indirubinoxime
FAK	Focal adhesion kinase
FDA	Food and drug administration
FGF	Fibroblast growth factor
FOXO	Forkhead family of transcription factors

G

GAP	GTPase activating protein
Glu	Glutamate
GPCR	G-protein coupled receptor
Grb	Growth factor receptor binding protein
GSK-3β	Glykogen synthasae kinase-3β

H

HDAC	Histon deacetylase
HDL	High density lipoprotein
HEPES	N-(2-hydroxyethyl)piperazine-N‘-(2-ethansulphonic acid)
HER	Human epidermal growth factor receptor
HRP	Horse reddish peroxidase

I

I3MO	Indirubin-3‘-monoxime
ICAM-1	Intercellular adhesion molecule 1
IFN-γ	Interferon-γ
IGF	Insulin-like growth factor
IgG	Immunglobulin G
IHD	Ischemic heart disease
IκB	Inhibitory subunit of NF-κB
IKK	IκBα kinase
IL-1	Interleukin-1

J

JAK	Janus kinase
JNK	c-Jun N-terminal kinase

K

kDa	Kilo Dalton

L

LDL	Low density lipoprotein

M

MAPK	Mitogen activated protein kinase
mc	Monoclonal
Mcl-1	Myeloid leukaemia-1
MCF-7	Human mammary carcinoma cell line
MCP-1	Monocyte chemotactic protein-1
MEF	Mouse embryonic fibroblasts
MeOH	Methanol

N

5‘-NIO	5‘-nitro-indirubinoxime
NADH	Nicotinamide adenine dinucleotide
NADPH	Nicotinamide adenine dinucleotide phosphate
NF-κB	Nuclear factor-κB
NO	Nitric oxide
NRTK	Non-receptor tyrosine kinase

P

p-Tyr	Phospho-tyrosine
PAA	Polyacrylamide
PBS	Phosphate buffered saline
pc	Polyclonal
PC	Proprotein convertase
PCAM-1	Platelet cellular adhesion molecule-1
PDGF	Platelet-derived growth factor
PDGFR	Platelet-derived growth factor receptor
PDK	Phosphoinositide-dependent protein kinase
Ph^+	Philadelphia chromosome positive
PH-domain	Pleckstrin homology-domain
$PI(3,4,5)P_3$	Phosphatidylinositol-3,4,5-triphosphate
$PI(4,5)P_2$	Phosphatidylinositol-4,5-bisphosphate
PI3K	Phosphatidylinositol 3-kinase
PK	Protein kinase
PLC	Phospholipase C
PMSF	Phenylmethylsulphonylfluoride
PTEN	Phosphate and tensin homologue deleted on chromosome ten
PTP	Protein tyrosine phosphatase
PVDF	Polyvinylidenefluoride

R

Rb	Retinoblastoma protein
RLU	Relative light unit
ROS	Reactive oxygen species
RTK	Receptor tyrosine kinase

S

SAPK	Stress-activated protein kinase
SDS	Sodium dodecyl sulphate
SDS-PAGE	Sodium dodecyl sulphate polyacrylamide gel electrophoresis
Ser	Serine
SFK	Src-family kinase
SH2/3/4 domain	Src-homology 2/3/4 domain
Shb	Src-homology 2 domain containing adaptor protein B
SHP	SH2-containing protein-tyrosine phosphatase
SMC	Smooth muscle cell
SOCS	Suppressor of cytokine signalling
Sos	Son of sevenless
STAT	Signal transducer and activator of transcription
STATRE	STAT-specific response element

T

T	Threonine
5‘-TAIO	5‘-trimethylacetamino-indirubinoxime
TAK-1	Transforming growth factor-β-activated kinase 1
TBS-T	Tris-buffered saline containing Tween 20
TCDD	2,3,7,8-tetrachlorodibenzo-p-dioxin
TCM	Traditional Chinese medicine
TEMED	N,N,N‘,N‘-tetramethylethylene diamine
TGF	Transforming growth factor
Thr	Threonine
TKRB	Tyrosine kinase reaction buffer
TNF	Tumor necrosis factor
tPA	Tissue plasminogen activator
TRAF	TNF receptor associated factor
Trolox	6-Hydroxy-2,5,7,8-tetramethylchromane-2-carboxylic acid
Tyr	Tyrosine

V

VCAM-1	Vascular cellular adhesion molecule-1
VEGF	Vascular endothelial growth factor
VLDL	Very low density lipoprotein
VSMC	Vascular smooth muscle cell

Y

Y	Tyrosine

2. Curriculum Vitae

Personal Data

Name:	Christoph GROJER
Date of birth:	27.08.1984
Place of birth:	Vienna
Nationality:	Austrian

Education

09/1990 – 06/1994	Elementary school: “Notre Dame de Sion“, Vienna
09/1994 – 06/2002	Grammar school: „Bundesrealgymnasium Wien 7“, Vienna
10/2003	Inscription at the University of Vienna Diploma study in pharmacy
03/2008 – 09/2008	Diploma thesis at the “Molecular Targets“ group, Department of Pharmacgnosy, University of Vienna

Further Activities

10/2002 – 06/2003	Basic military service „van-Swieten Kaserne“, Vienna

3. Acknowledgements

Initially I would like to thank Univ.-Prof. Dr. Verena Dirsch for giving me the chance to perform my diploma thesis in her “Molecular Targets“ group at the Department of Pharmacognosy, University of Vienna.

Furthermore I want to express my gratitude to all current and former members oft he “Molecular Targets“ group for their enormous helpfulness with all emerging problems during my diploma research, as well as fort he very professional but still relaxed atmosphere in the lab. I am also very grateful tot hem for numerous common activities and amusement outside the lab.

At this point I also want to mention Mr. Alexander Heinrich, who performed his diploma research the same time I did. I want to thank him for various memorable experiences inside the lab, as well as for incidental recreative get-together with friends at a drink after work.

I also want to express my sincere thanks to Dr. Andrea Schwaiberger, my tutor during my time at the “Molecular Targets“ group, not only for teaching me all necessary knowledge and skills which form the basis of this work, but also for her incredible patience, enthusiasm, helpfulness and dedication which I experienced during our common time in the lab as well as during subsequent completion of this work.

I warmly thank all of my friends, relatives and family members, which accompanied and supported me during my study period and previous stages of my life.

Finally I want to express my dearest thanks to my parents for their unconfined support and unreserved encouragement which they paid to me throughout my entire life. I am also very grateful to them for always encouraging me to follow and achieve my goals.